CHARACTERIZATION AND IMPLEMENTATION OF BATTERY MANAGEMENT SYSTEM

BY

ABDELHAMED TARIG ABDELHAMED MOHAMED

A Thesis Presented to the
DEANSHIP OF GRADUATE STUDIES

KING FAHD UNIVERSITY OF PETROLEUM & MINERALS

DHAHRAN, SAUDI ARABIA

In Partial Fulfillment of the
Requirements for the Degree of

MASTER OF SCIENCE

In

ELECTRICAL ENGINEERING

May 2018

KING FAHD UNIVERSITY OF PETROLEUM & MINERALS

DHAHRAN- 31261, SAUDI ARABIA

DEANSHIP OF GRADUATE STUDIES

This thesis, written by **ABDELHAMED TARIG ABDELHAMED MOHAMED** under

the direction of his thesis advisor and approved by his thesis committee, has been presented

and accepted by the Dean of Graduate Studies, in partial fulfillment of the requirements

for the degree of **MASTER OF SCIENCE IN ELECTRICAL ENGINEERING.**

Dr. Mohammad A. Abido
(Advisor)

Dr. Ali A. Al-Shaikhi
Department Chairman

Dr. Ibrahim M. El-Amin
(Member)

Dr. Salam A. Zummo
Dean of Graduate Studies

Dr. Mohammad M. Al-Muhaini
(Member)

22/11/13

Date

© Abdelhamed Mohamed

2018

Dedication

To my Father

For every word of wisdom, you said…

For every road of greatness, you showed…

For your guidance and support,

Through sickness and health, and in poor or wealth,

Dear Father, Mr. Tarig Abdelhamed,

Thank you, for EVERYTHING.

Without your sacrifice, this master's degree would not reach to its final steps, this step.

And for that, I dedicate this work to YOU.

ACKNOWLEDGMENTS

From the beginning to the end, from the word 'GO', and through every high and low in the period of this thesis, a lot of remarkable unpresented gentlemen had helped and guided me to overcome everyday challenges and obstacles, to accomplish the desired mission of producing a meaningful piece of work. To whom, a word of thanking is not even enough to express the amount of gratitude they deserved.

First and foremost, a special amount of gratitude and gratefulness to my thesis advisor Prof. *Mohamed Abido*, who throughout my work had shown me the patience and knowledge in his mentorship and guidance throughout this journey, to produce a novel work of research.

I'd like to express my deepest thankfulness and appreciations to my committee members, Prof. Ibrahim M. El-Amin and Dr. Mohammad M. Al-Muhaini, for their remarks and recommendation in this research.

TABLE OF CONTENTS

LIST OF TABLES

LIST OF FIGURES

LIST OF ABBREVIATIONS

Ah	Amp-hour
AKF	Adaptive Kalman Filter
ANN	Artificial neural network
BESS	Battery energy storage system
BES	Battery energy storage
BMS	Battery management system
C	Current rate
CC	Constant current
CC-CV	Constant-current constant-voltage
DEKF	Double Extended Kalman Filter
EKF	Extended Kalman Filter
EV	Electric vehicle
KF	Kalman Filter
OCV	Open-Circuit Voltage
SOC	State of Charge
RTDS	Real Time Digital Simulator

ABSTRACT

Full Name   : ABDELHAMED TARIG ABDELHAMED MOHAMED

Thesis Title   : CHARACTERIZATION AND IMPLEMENTATION OF BATTERY MANAGEMENT SYSTEM

Major Field   : ELECTRICAL ENGINEERING

Date of Degree : May 2018

The security, operation reliability along with the assurance of optimal charging of any battery energy storage system (BESS), are the main objectives and the key features of the battery management system (BMS). This thesis proposed a modern technique in controlling the charging of the battery by estimating and monitoring the state of charge (SOC), starting by considering one of the most complex and sophisticated battery model, that imitates the battery in real life, which is the second-order RC battery model, that uses the Open Circuit Voltage (OCV) in order to estimate the SOC. In addition to that, the model was enhanced with the introduction of hysteresis effect that would imitates the previous charging history. The Kalman Filter is a robust method that is widely applied in modern BMS by researchers, which can provide real time estimation for both battery parameters and states. In this thesis the Double Extended Kalman Filter (DEKF), which is the nonlinear form of the KF is used to determine battery's impedance parameters, as well as the battery's SOC. By combining the proposed model, with the power of DEKF to identify the circuit parameters and the estimation of SOC it was possible to develop more reliable and robust charging system. The efficiency of the proposed control strategy was confirmed through MATLAB simulation, along with the validation using Real Time Digital Simulator (RTDS) based system to achieve the best control of BESS within the required SOC.

ملخص الرسالة

الاسم الكامل: عبدالحميد طارق عبدالحميد محمد

عنوان الرسالة: تحديد خصائص و تطبيق نظام إدارة للبطاريات

التخصص: الهندسة الكهربائية

تاريخ الدرجة العلمية: مايو 2018

يعتبر الأمان وموثوقية العمليات وضمان الشحن الأمثل لأي نظام تخزين للبطارية هي الأهداف الرئيسية والميزات الرئيسية لنظام إدارة البطارية. اقترحت هذه الورقة تقنية حديثة للتحكم في شحن البطارية من خلال تقدير ومراقبة حالة الشحن ، بدءاً من النظر في واحدة من أكثر نماذج البطاريات تطوراً وتعقيداً التي تقلد البطارية في الحياة الحقيقية ، وهو نموذج المستوى الثاني المكون من مقاومة ومكثف ليمثلا البطارية ، والذي يستخدم جهد الدائرة المفتوحة من أجل تقدير حالة الشحن للبطارية. بالإضافة إلى ذلك ، تم تعزيز النموذج بإدخال تأثير التباطؤ الذي سيقلد تاريخ الشحن السابق.

مرشح كالمان هو طريقة قوية يتم تطبيقها على نطاق واسع في نظم إدارة البطاريات الحديث من قبل الباحثين ، والتي يمكن أن توفر تقديرًا في الوقت الفعلي لكل من معلمات البطارية والحالات. في هذا البحث ، تم استخدام مرشح كالمن المقدّم المزدوج ، وهو شكل غير خطي من مرشح كالمان الأساسي ، لتحديد معلمات مقاومة البطارية ، بالإضافة إلى حالة شحن للبطارية. من خلال الجمع بين النموذج المقترح ، مع قوة مرشح كالمن المقدّم المزدوج لتحديد معلمات الدائرة وتقدير مستوى الشحن ، كان من الممكن تطوير نظام شحن أكثر موثوقية وقوة.

تم التأكيد على فعالية استراتيجية التحكم المقترحة من خلال محاكاة في برنامج ماتلاب ، إلى جانب التحقق من الصحة باستخدام نظام المحاكاة في الوقت الحقيقي لتحقيق أفضل تحكم في نظام تخزين للبطارية ضمن مستوى الشحن المطلوب.

CHAPTER 1

INTRODUCTION

1.1   Overview

The development and emerging of battery energy storage systems (BESS), have shown an enormous upgrade in the last couple of years. Ranging from the small level of power, as in the portable cell phone devices, to the recently developed super capacitors, that could serve as a backup system for AC or DC Microgrid. The reliability and feasibility study for such storage system had been confirmed in such recent studies [1]–[3], which shows how the addition of battery in a microgrid system could help in major utilization of renewable energy systems. Also, on the low power level, the new smartphone have shown their durability for long periods of times, from companies such as Lenovo that was able to produce a battery that could work up to 1730 minutes, and Huawei where their best battery phone reach to 1600 minutes of working [4].

One of the most utilization of storage systems capabilities is the development of the electric vehicles (EV). Recently rising environmental concerns, had obligate societies to came up with substitutions to the conventional combustion engines as source of power for vehicles. Ecological concerns that include both the effect on the health caused by emissions of exhaust gas, along with increasing level of CO_2 emissions which the lead reason for global

warming. With recent advancement in batteries storage systems, the EVs are now being mass produced and sold commercially [5].

A requirement to these applications is a management system, which could be considered as the core or the brain of the battery, where it's able to control and monitor every aspect of the battery's operation to ensure that the battery is working in the optimum operating envelope. Battery management systems (BMS) become a necessity for most battery technologies, not to ensure the safely operation alone, but also support the battery to achieve its maximum power and energy capabilities, without operating above the recommended restrictions. In order to achieve these objectives, BMS takes into its responsibility to perform these following tasks: data acquisition, Cell protection, Thermal management and Battery state monitoring. Data acquisition is important to collect the most relevant measurements for the battery, which are the voltage and current, and to notice and capture the significant transient effects, these measurements should be collecting in appropriate sampling frequencies. Battery cell protection techniques have been developed by recent researches [6] [7]; to ensure that the battery will not violate its safe operation area (SOA) which leads to prolong the service lifetime of the battery. Moreover, researcher at [8] showed that in order to combine the high performance of a battery with the extension of its lifetime along with the optimal operation; an effective thermal control on the battery must be available.

To design a powerful, robust management system for battery storage system, the online identified of several battery states is needed. The time-variability nature of the characteristics of any battery, which include the battery's State of charge (SOC), along with the impedance parameters, are the main challenges in monitoring the states of the

battery, and that's because of effect of time on the battery that's leads to its ageing, in addition to varying operating conditions on the battery [9]. Hence, to produce a reliable and accurate set of battery state estimates; the selected controlling system must adaptively correct the variations.

1.2   Research Motivation

Controlling the estimated state of charge (SOC) for battery energy storage systems (BESSs) is the main challenge behind increasing battery use power applications.

The poor estimation of a SOC and a BESS control can result in problems with unwanted over discharge and overcharge of the battery, lower efficiency of operation, and reduced battery life.

Convectional control schemes have shown its drawbacks in its inability to cope with online estimation, along with its significant increase in the cost of the additional memory consumption along with high computational power when some of the modern method were proposed.

Providing the optimum model along with fast, and appropriate control scheme will lead to overcome and prevent these drawbacks, and lead to more reliable and secure system.

1.3   Thesis Objectives

The prime objective of this research is to design a robust battery management system, by first, selecting a dynamic model that would represent the real-life battery, which the second order RC model with the introduction of the hysteresis effect. This model would be used to identify the battery's impedance parameters for every step of the time. Thereafter, the open circuit voltage (OCV) predication is made using the structure of the dynamic model, which is then applied to a predefined function in order to estimate the SOC. The estimation throughout the thesis would be done using an advanced version of the Kalman Filters techniques which is the Double Extended Kalman Filter (DEKF). The robustness of the recursive Kalman Filter set of equations made it a viable option for any dynamic system to be identified stochastically. To validate the controller performance, non-linear simulation is carried out using MATLAB. Figure 1-1 illustrates and summarize the requirement of the proposed battery management system.
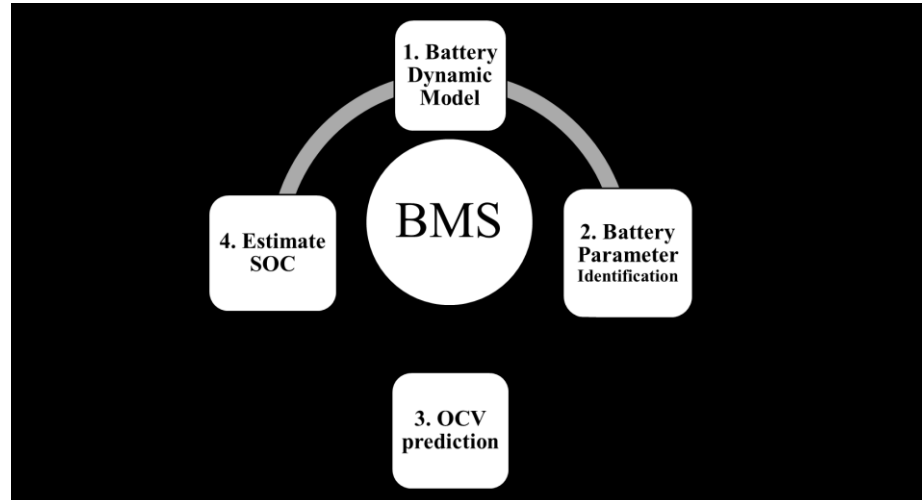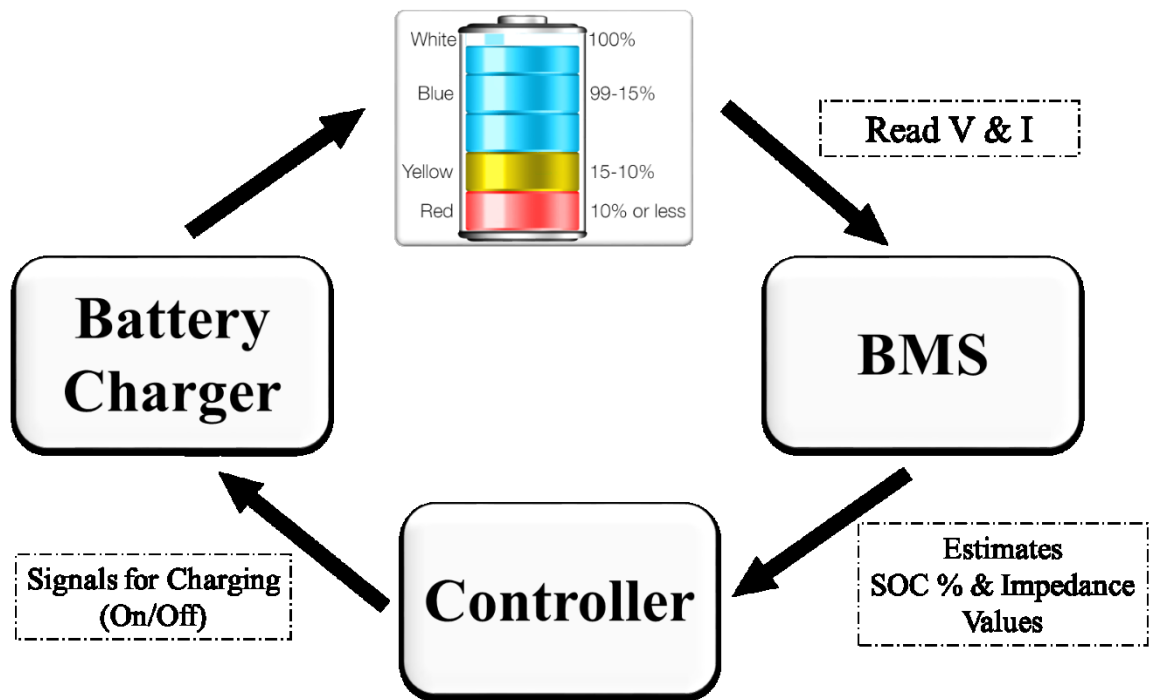
Figure 1-1:Charging cycle and the tasks of the Battery Management System

1.4   Thesis Contributions

This paper proposed a modern technique in controlling the charging of the battery by estimating and monitoring the state of charge (SOC), starting by considering one of the most complex and sophisticated battery model, that imitates the battery in real life, which is the second-order RC battery model, that uses the Open Circuit Voltage (OCV) in order to estimate the SOC. In addition to that, the model was enhanced with the introduction of hysteresis effect that would imitates the previous charging history.

The Double Extended Kalman Filter (DEKF) will be adopted, where we could use the estimated SOC as one of the inputs to the system, in addition to the ability of making the estimation of the nonlinear model happened in real time.

1.5   Thesis Breakdown

Chapter 2 presents a relevant background and literature review which includes a detailed explanation of all aspect of the Battery Management System (BMS). The modeling of proposed system and the procedure of the controller design is addressed in chapter 3. Chapter 4 discusses the outcome results from all the considered scenarios with a comparison between the simulation and the RTDS results. Chapter 5 concludes the thesis and offers some ideas that could be applied in future.

CHAPTER 2

BACKGROUND AND LITERATURE REVIEW

2.1   Background

Battery devices are becoming the favorite choice for electrical energy storage and supply in a wide range of motive and stationary power applications. Without significant improvements in battery technologies and battery management systems, the future uptake of these electrochemical energy storage devices will remain a challenge.

The environmental concerns over the emissions of greenhouse gases, together with the volatile and ever-increasing prices of fossil fuels have led to the large-scale adoption of battery devices in the transport and utility sectors. These motives, together with the recent advances in electrochemistry science and manufacturing techniques have resulted in numerous battery technologies, each having their own specific performance capabilities.

In these section, a brief remark for one of the most famous battery technology will be introduced, which is the lithium-ion battery. Thereafter, an overview for the battery management system in general and its tasks will be presented.

2.1.1 LITHIUM-ION BATTERY

Taking the fact that, Lithium has the highest electrochemical potential, along with the properties of being the lightest metal with largest energy density per weight of all metals found in nature, made it commonly used as the anode in the batteries, which lead to have batteries with excellent capacity ,high voltage and a remarkably high-energy density [10].

Lithium ion batteries are considered the most famous kind of batteries when it comes to portable ones. It takes almost over the half share of small portable devices market. It was first introduced to the world in 1960s, but the first commercial one was developed by SONY in 1990 [11]. Since then, the fast improvement in science of materials led to vast development in Li-ion batteries in terms of energy density which raised from only 75 Wh/kg to 200 Wh/kg, and also the cycle life has increased to reach 10,000 cycles. In addition to that, the most important advantage of Li-ion batteries over the other types is their efficiency, which may reach up to 100% [12].

Li-ion holds the highest potential for upcoming advance and optimization. the highest storage efficiency along with large energy density, in addition to low weight and small size; that what Li-ion batteries are able to offer, and that what made them ideally suitable for portable devices. Yet, some of the main weaknesses of Li-ion technologies are its excessive high price, and the damaging effect on its lifetime that deep discharging has on it [13].

The Li-ion battery has relatively high power/energy densities and specific power/energy, which has resulted in the current broad range of development, particularly in small-scale

Electrical Energy Storage (EES) applications. The cycle efficiencies of EES technologies have been continuously improved with time through development efforts leading to technology breakthroughs, and most commercialized techniques normally have medium-to-high cycle efficiencies. The energy capacity and the self-discharge of EES systems are the major factors in deciding the associated suitable storage duration [14].

Throughout its lifespan, the lithium-ion battery needs nearly no maintenance, which is a benefit that other batteries don't have. In addition to that, there is no memory effect and no arranged cycling is needed. Furthermore, and due to the fact that the lithium-ion battery has a self-discharge rate which is less than half of the discharge rate of lead-acid and NiMH batteries; that makes it well suited for electric vehicles [15]. Even with the plus-points of lithium-ion batteries, they also have certain downsides.

Lithium ions are fragile. To sustain the safe process of these batteries, they need a protecting device to be constructed into each pack. This device, also denoted to as the battery management system (BMS), limits the peak voltage of each cell during charging and stops the cell voltage from reducing underneath a threshold during discharging. The BMS also controls the maximum charging and discharging currents and monitors the cell temperature [11].

The most important parameters that determine the performance of lithium-ion cells are the operating temperature and voltage [16]. Figure 2 shows that the cell operating voltage, current and temperature must be kept within the area indicated by the green box labeled "Safe Operation Area" (SOA) at all times [17].

The cell could be permanently damaged if it is operated outside the safety zone. The batteries could be charged above its rated voltage or be discharged under the recommended voltage. If the recommended upper limit of 4.2 V was exceeded during charging, excessive current would flow and result in lithium plating and overheating. On the other hand, overly discharging the cells or storing the cells for extended periods of time would cause the cell voltage to fall below its lower limit, typically 2.5 V. This could progressively break down the electrode.

Over the past decade, lithium-ion batteries have achieved significant penetration into various markets, where high specific energy and power densities are desirable. There are several types of lithium-ion batteries in commercial use, such as, lithium cobalt oxide (LCO), lithium-ion iron phosphate (LFP), lithium-ion nickel manganese cobalt oxide (NMC), lithium nickel cobalt aluminum oxide (NCA) and lithium-titanite (LTO).

Whilst LCO batteries dominate the portable consumer electronics market, LFP and NMC batteries are gaining popularity amongst EV/HEV designers. In contradiction to LFP and NMC batteries, NCA batteries have a less favorable performance, especially at low temperatures where the power and energy capabilities are reported to be considerably lower.

Due to their more stable lithium-titanite anode structures, LTO batteries are the safest type of lithium-ion batteries available in the market, which can achieve faster charge times and higher discharge currents.

As a result, LTO batteries are now being considered for large-scale grid-tie energy storage applications, such as, load balancing, peak shaving and improving the frequency response of the grid.

The high levels of ongoing academic and industrial research on lithium-ion batteries, together with the advancements in manufacturing techniques are setting the tone for an increasing trend in large-scale adoption of lithium-based batteries. Therefore, this particular chemistry is chosen as the subject of study in this thesis, with a view to later develop an online state monitoring system for the commercially available NMC and LFP cells. It is worth noting that the algorithms developed in this thesis are also applicable to other battery chemistries, given knowledge of certain battery model parameters are available at initialization step.

2.1.2 BATTERY MANAGEMENT SYSTEMS (BMS)

In most real-world applications, a single cell will not be able to generate enough power to complete a given task. Therefore, battery packs, consisting of many cells connected in series and/or parallel formations are designed to achieve specified power and energy outputs. In order to keep the cells within their recommended operating envelope, battery management systems (BMS) are usually integrated into the pack design, serving as the "brain" of the battery system. Most battery technologies require a BMS to not only ensure a safe operation, but also to help the battery perform at its highest energy and power capabilities, without violating the recommended operating limits.

While the definition of a BMS could differ depending on the application, the basic task of the BMS could be defined in the following manner:

- It should ensure that the energy of the battery is optimized to power the product.

- It should ensure that the risk of damaging the battery is minimal.

- It should monitor and control the charging and discharging process of the battery.

According to the definition, the basic tasks of the BMS are identical to its objectives. Although different types of BMS have different objectives, the typical BMS follows three objectives:

- It protects the battery cells from abuse and damage.

- It extends the battery life as long as possible.

- It makes sure the battery is always ready to be used.

In some details, the function of the BMS could be summarized as follows:

1) Discharging control

The primary goal of a BMS is to keep the battery from operating out of its safety zone. The BMS must protect the cell from any eventuality during discharging. Otherwise, the cell could operate outside of its limitations.

2) Charging control

Batteries are more frequently damaged by inappropriate charging than by any other cause. Therefore, charging control is an essential feature of the BMS. For lithium-ion batteries, a 2-stage charging method called the constant current – constant voltage (CC-CV) charging method is used.

During the first charging stage (the constant current stage), the charger produces a constant current that increases the battery voltage. When the battery voltage reaches a constant value, and the battery becomes nearly full, it enters the constant voltage (CV) stage. At this stage, the charger maintains the constant voltage as the battery current decays exponentially until the battery finishes charging.

3) State-of-Charge Determination

One feature of the BMS is to keep track of the state of charge (SOC) of the battery. The SOC could signal the user and control the charging and discharging process. There are three methods of determining SOC: through direct measurement, through coulomb counting and through the combination of the two techniques.

4) State-of-Health Determination

The state of health (SOH) is a measurement that reflects the general condition of a battery and its ability to deliver the specified performance compared with a fresh battery. Any parameter such as cell impedance or conductance that changes significantly with age could be used to indicate the SOH of the cell. In practice, the SOH could be estimated from a single measurement of either the cell impedance or the cell conductance.

5) Cell Balancing

Cell balancing is a method of compensating weaker cells by equalizing the charge on all cells in the chain to extend the overall battery life. In chains of multi-cell batteries, small differences between the cells due to production tolerances or operating conditions tend to be magnified with each charge discharge cycle. During charging, weak cells may be overstressed and become even weaker until they eventually fail, causing the battery to fail prematurely.

6) Logbook Function

Because the SOH is relative to the condition of a new battery, the measurement system must hold a record of the initial conditions or a set of standard conditions for comparison. An alternative method of determining the SOH is to estimate the SOH value based on the usage history of the battery rather than on certain measured parameters, such as the number of charge-discharge cycles completed by the battery. Therefore, the logbook function of the BMS would record such important data to the memory system.

2.2 LITERATURE REVIEW

This part will provide an overview of the state of art and related studies about the state of charge estimation techniques, the advantages of each technique and its drawbacks.

In addition to that, Battery Impedance Characterization Methods will be discussed and hence the proposed enhancement would be proposed to overcome all the obstacles.

2.2.1 SOC Estimation Algorithms

State of charge estimation is one of the important parameters that are essential to guarantee secure charging and discharging. SOC is defined as the current charge capacity with respect to its rated capacity [37][38], and it's being represented by percentage. To let the batteries safely charged and discharged at appropriate level, that would enhance the battery's lifetime, SOC must provide the present state of the battery with accurate values, that would help in the battery management.

Nevertheless, calculating SOC is not a straight forward mechanism, since it includes the measurement of battery current, voltage, temperature and any other information that might affects to the battery under consideration. Precise estimation of SOC avoids battery damage or quick aging by preventing inappropriate overcharge and over discharge. Figure 2-1 illustrates the state of charge estimation methods, and the dark bolded line represents the path that have been followed throughout this thesis.
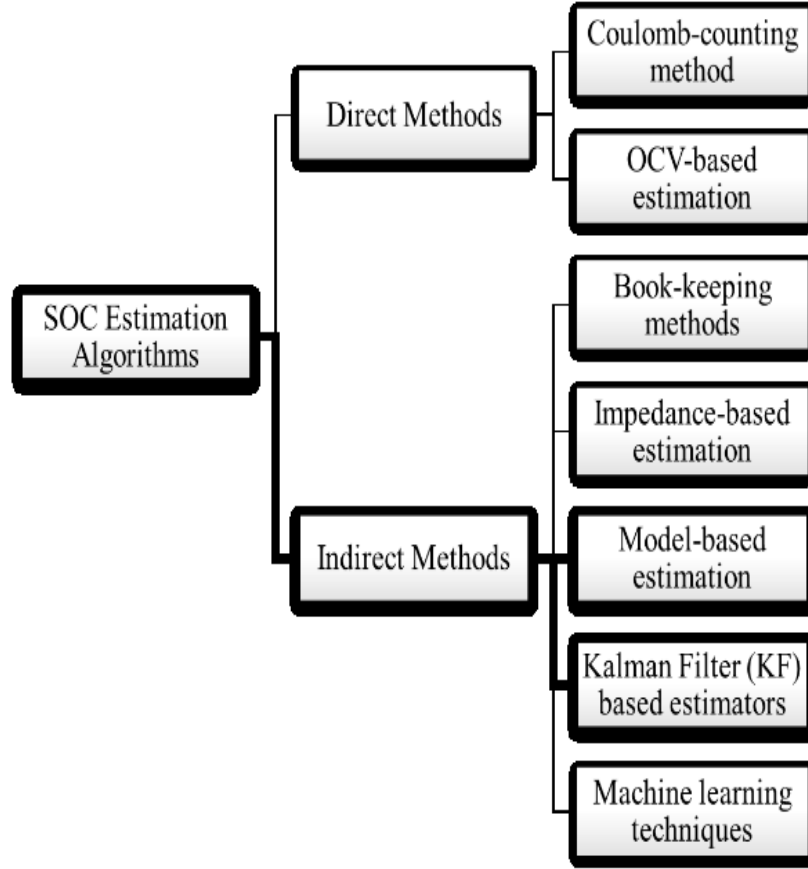
Figure 2-1: SOC Estimation Algorithms

A. Coulomb-counting method

Coulomb-counting is a straightforward implementation technique for the estimation of SOC, when a preliminary value noted as SOC (t_0) is given, and by taking the time integral of the terminal current, a charge indicator for the battery could be available, as shown in Equation (1).

$$SOC(t) = SOC(t_0) - \frac{\eta}{Q_{nom}} \int_{t_0}^{t} I(\tau).d\tau \qquad (2\text{-}1)$$

Where the current of the battery is represented as $I(\tau)$, η is for charging and discharging where its value would be $= 0$, for discharging, and for charging it would be $\eta<1$. Q_{nom} represents the battery's coulombic efficiency, and could be written with respect to battery's nominal capacity in ampere-hours C_{nom} using this formula: $Q_{nom}=C_{nom}\times3600s$. The conventional Coulomb counting SOC Estimation technique has a weak point from error accumulation glitch, which lead to wrong states predictions[39], [40].

B. OCV-based estimation

Battery's SOC estimation could be done by the relation of the SOC with the battery's OCV as shown in figure 2-2. The major drawback for this technique is the fact that in order to establish an OCV measurement; the no-load connection time must be very long, which make it not suitable for online application. In addition to that, this technique showed unstable SOC estimation for batteries with flat OCV curves [41].

These weaknesses have given an opportunity for more advanced SOC estimation techniques to emerge, in which a dynamic model representation for the battery could be employed in order to utilize the parameters for predicting an accurate battery states. One of the methods that was proposed in the literature to plot the OCV relaxation time against time was using a semi-log scale, from which the OCV is estimated as a logarithmic function [42]. However, the ageing problem of the battery made the estimation of the parameter unreliable. To solve this problem, adaptive SOC techniques were developed, in which an

exponential function was proposed for the estimation [43], which was even more enhance by the work of [44] at which a more sophisticated empirical model was used.
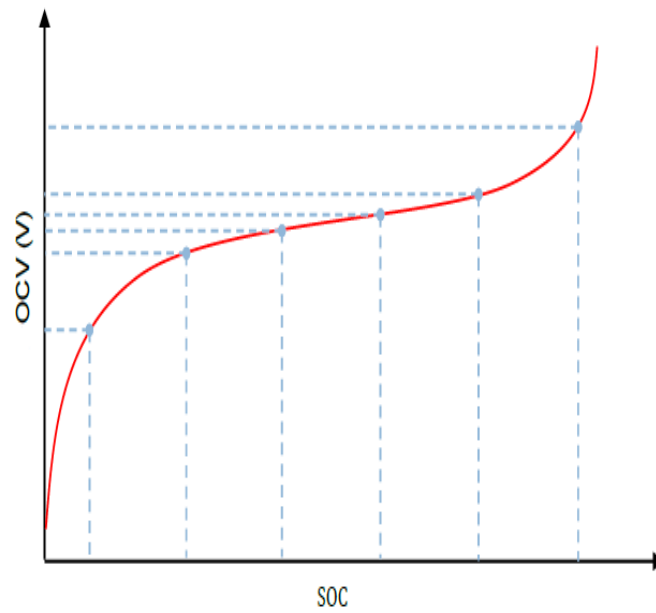
Figure 2-2: Relationship Between OCV & SOC

C. Book-keeping method

For online battery management system implementation, a look-up tables are used in the book-keeping method in order to relate the SOC with battery characteristics. In [18] and [19] a technique was proposed to link the current, temperature and the voltage of the battery with the SOC estimation, using a predefined function. Despite its simplicity, and due to the fact that the effect of battery aging is not considered and the stored function can only work for the characterized battery; it's not practical to use book-keeping SOC estimation for dynamic power implementations.

D. Impedance-based estimation

This method have been widely used for SOC estimation for different types of batteries [47]–[49]. This method could be considered similar to OCV-based method. However, in this approach, a relationship between the impedance and the SOC is replacing the OCV-SOC look-up table. The major drawbacks for this method is its inability to provide precise SOC estimate with the ageing of the battery, along with its sensitivity to temperature, that lead to low accuracies when it comes to SOC estimation [50], [51].

E. Model-based estimation

This method is considered one of the most used techniques in SOC estimation, and many researchers are adopting it throughout their recent studies on BMS[52]–[54]. As the name says, the method aims to implement a representation for the battery by modeling it into a

deterministic model. The more complex and sophisticated the model is, the more accurate and realistic the estimations from the model would be, as the model will be nearly similar to real life battery. The main objective is to come up with a representation that could relate the battery terminal parameters, such as current and voltage, to the SOC of the battery [52]–[56]. The inputs to the system calculate the OCV of the battery throughout the operation, which then would be used with SOC-OCV relationship to provide a real-time estimation for the SOC. Similar to OCV method, the lifetime of the battery affects the parameters of the estimation algorithm. Also, the more complex the model, the more difficult the adaptation of the parameters will be. Despite that, the popularity of this method is increasing in battery characterization, in applications is which the operation of the battery couldn't be interrupted.

This method would be adopted in this thesis. However, and in order to overcome its drawbacks; it would be combined with the next presented method of estimation, the Kalman Filter (KF) based estimators.

F. Kalman Filter (KF) based estimators

The robustness of the recursive Kalman Filter set of equations made it a viable option for any dynamic system to be identified stochastically [57]. It became widely used throughout many applications, including the management of battery systems. The standard KF is normally used with linear and simple battery models. In [58], [59] the KF method was used by the authors to obtain the OCV of the battery and then using it to predict the value of SOC. However, in order to compensate for the nonlinearity nature of the complex models

of the battery systems, an upgraded level of the standard KF is used. The most famous type of the nonlinear KF is known as the Extended Kalman Filter (EKF). Due to its popularity, many research have adopted this technique in their studies on BMS [60]–[67]. From these studies, it could be argued that the EKF have a weakness towards the measurement noises along with minor linearization inaccuracies, which the effect of the battery ageing plays a major role in it. On top of that, the main drawback for all the KF-based estimators is the fact that, inaccurate initial condition set or a priori knowledge of parameters could lead the results to be diverged or it might converge very slowly.

To overcome these major problems, in this thesis the Double Extended Kalman Filter (DEKF) will be adopted, where we could use the estimated SOC as one of the inputs to the system, in addition to the ability of making the estimation of the nonlinear model happened in real time. Although there are some other developed KF as Sigma-Point KF (SPKF), Central-Difference KF (CDKF) and Unscented KF (UKF), whose have been validated for state estimation for batteries, yet they have shown a significant increase in the cost of the additional memory consumption along with high computational power [68]–[71].

G. Machine learning techniques

Throughout the last decade, machine learning methods had found their way probably into any application in real life, one of the is the management of battery systems. The most notable techniques in BMS and their application in the state estimation are fuzzy logic (FL) [45][46], and Artificial neural networks (ANNs) [47][48]. Implementation wise, these techniques are similar to the model-based methods which have been described previously,

but rather than representing the SOC in a deterministic model, it could be done using ANNs as an example. The major benefit that come out of such techniques is that it's not a requirement for the battery parameters to have a priori knowledge. Nevertheless, and because of the fact that these methods require a diversified and enormous forms of datasets, a considerable amount of over-fitting and probably required a huge computational power, they found to be not usually applicable for online battery management system applications that its main objective is to be designed at low-cost controllers. In addition to that, these techniques find it difficult to adapt to manufacturing variations and the ageing of the battery; and that's because of the open-loop nature of these methods.

2.2.2 Battery Impedance Characterization Methods

In modern battery monitoring systems, impedance parameters often serve as a good indicator and/or recalibration means for various battery states including SOC, state of health (SOH) and state of power (SOP). During operation, the impedance parameters can vary significantly due to both internal and external factors. The internal factors are the

battery's SOC, SOH and heat generation due ohmic losses, whilst the external factors may

include ambient temperature, current and previous history of battery usage [76] .
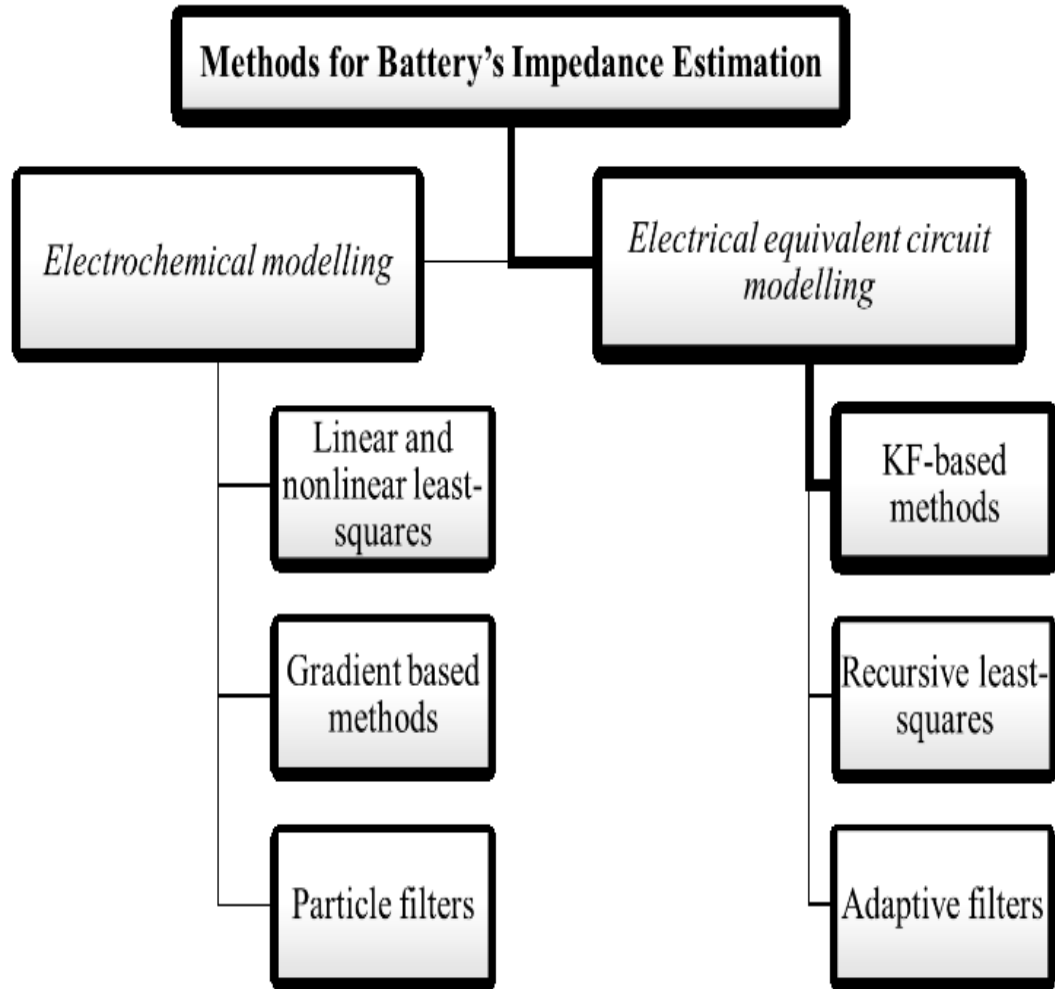
Figure 2-3: Methods for Battery's Impedance Estimation

As result, many reaches have been reported on both Electrochemical and electrical impedance characterization techniques, as summarized in Figure 2-3. But, on this thesis, the only desired and focused part will be on the electrical equivalent circuit modeling technique.

Electrical equivalent-circuit models have been found useful in many online battery state and parameter estimation algorithms. Figure 2-4 illustrates an exemplary simple equivalent-circuit model structure, where OCV is defined as a function of SOC, R_{int} represents the battery's total internal resistance and VT is the terminal voltage. By using such models, it is possible to relate the obtained battery parameters to real battery states, including SOP and SOH.

Figure 2-4: Simple electrical equivalent-circuit battery model

Moreover, due to their relatively simplified numerical approaches, equivalent-circuit models are highly desirable for online BMS implementations on low-cost microcontroller platforms. There are various techniques reported in literature that can be applied to equivalent-circuit models to extract the battery impedance parameters in real time. Some of the most sighted techniques are:

- KF-based methods;

- Recursive-least-squares methods;

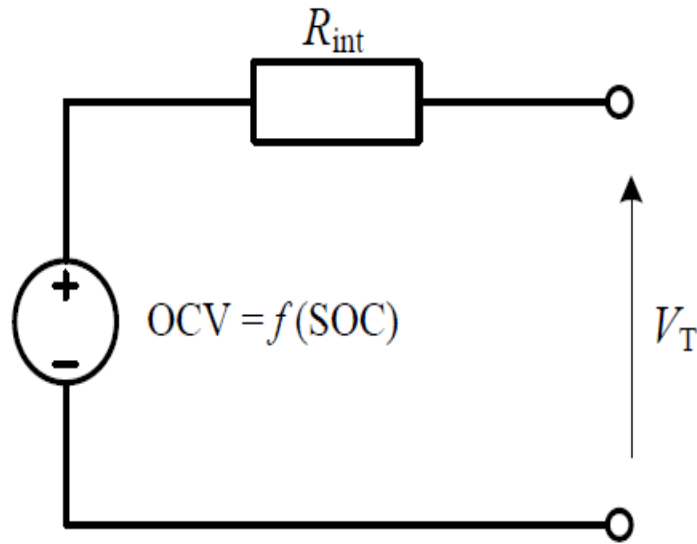- Other adaptive approaches.

KF-based methods are not only useful in online battery state estimation problems, but can also be implemented in different formats to simultaneously identify the battery's impedance parameters. For example, in [77]–[79], the authors adopt a joint EKF approach to real-time battery identification, where system unknowns are stacked up in a single EKF for simultaneous estimation of the model states and parameters. The disadvantage of joint EKF for online applications is the increased number of large matrix operations (e.g. matrix inversions) due to the high dimension of the augmented state model.

Hence, in this paper, the double EKF is employed in the BMS, to separate the process of state and parameter estimation by using two individual filters running in parallel. Due to the recursive nature of such system identification methods, the requirements for storage memory is very low; therefore, their implementations on low-cost controllers is achievable.

Least-squares techniques have also been applied to online battery parameter estimation problems. In [80]–[82], the authors have applied different variations of the least-squares

method, such as, recursive least-squares (RLS), recursive least-mean-squares (RLMS) and weighted RLS (WRLS) to identify different battery model structures in real time. Compared to KF-based approaches, these techniques are computationally less intensive. However, they are less robust in cases where persistence of excitation is poorly conditioned. In [83], a moving window least-squares approach to battery parameter estimation was taken in an effort to improve the filter's convergence. This was achieved at the expense of increased memory consumption for storage of battery data sampled in a 'window'.

In addition to KF-based and recursive least-squares methods, other adaptive approaches to online battery parameter identification have been reported. For example, in [84]–[86],a sliding-mode observer is proposed to estimate the battery parameters in real time. The use of evolutionary techniques for battery identification have also been reported in literature. These include genetic algorithms [87] and particle-swarm optimization methods [88]. Although higher estimation accuracies are achievable compared to least-squares-based methods, however, the requirements for tremendous computational power and memory consumption prevents these techniques from most online BMS applications.

2.2.3 Charging Methods

The Electric Power Research Institute (EPRI), which plays a leading role, and the Society of Automotive Engineers (SAE) categorize charging levels as alternating current (AC) Level 1, AC Level 2, and direct current fast charging (DCFC) Level 3, along with the subsequent functionality requirements and safety systems [18].

Types of charging systems A battery charger is a device used to transfer energy to a rechargeable EV battery by processing and controlling the electric current through it. An EV charger incorporates a rectifier to recharge an EV battery by converting AC to DC. Battery charging can be categorized based on the mode of energy transfer such as conductive or inductive, and the battery swapping types.

The traditional charging techniques include constant current (CC), constant voltage (CV), constant power (CP), trickle current(TC), and taper and float charging. An advanced charging technology recently combined the aforementioned techniques, resulting in CC-CV and pulse and reflex or negative pulse charging, which are utilized to charge batteries rapidly [19] [20], [21].

CC charging is the simplest technique; it employs a single low-level current to the discharged battery. In practice, the current level is set as 10% of the maximum rated capacity of the battery. This type of charging is best suited for nickel-cadmium and nickel-metal hydride batteries [22]. However, gassing and overheating may occur if the battery is over charged. Similarly, a small current is applied to recompense for the self-discharge of a battery in TC charging [19]. Taper charging utilizes unregulated CV charging, which may result in serious damage to the cells through overcharging. On the contrary, float charging

uses CV method below the upper limit of the battery. This charging system is usually used for emergency power back-up systems and is suitable for lead-acid battery[22].

In general, CC–CV charging technique is utilized for majority of commercial chargers to charge a lithium- ion battery because this battery has higher power and energy densities than others [20], [22], [23]. The advantages of the CC–CV technique include limited charging current and voltage through battery controller utilization. Thus, over-voltages are prevented and thermal stress is reduced. First, a CC is applied to charge a battery until a pre-defined voltage level is achieved, and then a CV is used until a termination condition is reached. CC charging mode is faster than CV charging mode. The charging time of a battery is one of the most important issues in the large deployment of EVs. Even though CV mode is used to charge the remaining battery capacity, the charging duration takes approximately the same amount of time or more time than CC mode due to a necessary decrease in charging current to help top-off the battery [22].

Many studies enhanced the standard CC–CV charging technique to reduce the charging time and increase battery capacity. For the same purpose, PC-based charging technique is also used in different studies. However, the current charging systems still have some limitations. Therefore, more studies are required on this issue for enhancement [18].

The profile of a 40 Ah, 105 V li-ion battery pack charging from 5% SOC to 95% SOC is shown in Figure 2-5. During the constant current charging phase, the charging current is fixed at 13.5 A. Once the pack voltage reaches 115.2 V, the controller then switches into

constant voltage charging, maintaining the pack voltage at 115.2 V; at this point, the

charging current begins to drop until the charging current falls below 1 A.
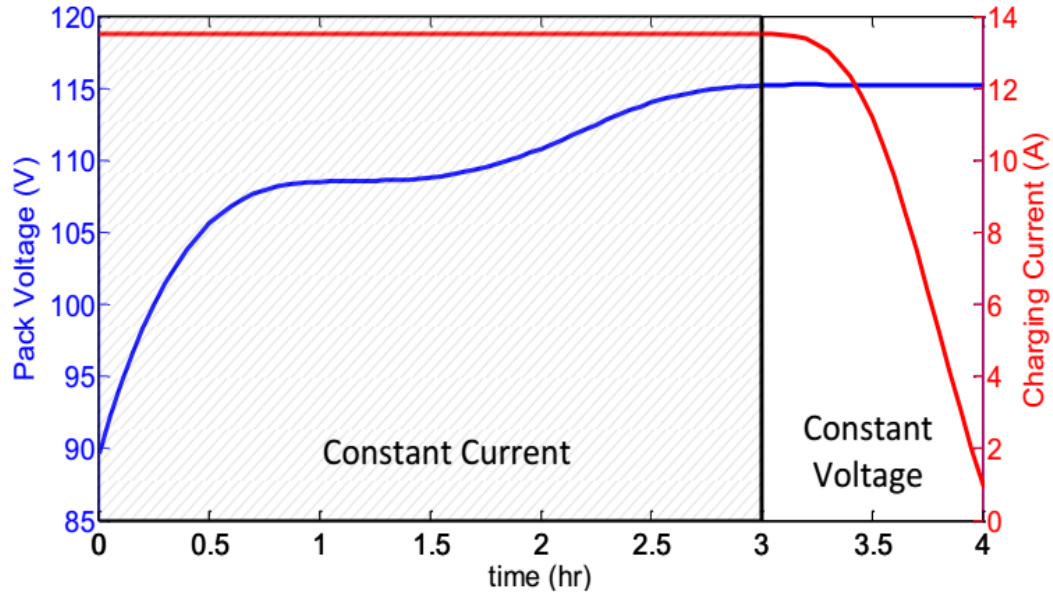
Figure 2-5: Charging profile of 40 Ah 32 cell, 105.6 V li-ion battery pack

Pulse-charging and negative pulse-charging are also good charging strategies for fast

charging of an EV battery [22]. Pulse-charging charges a battery by feeding charge current

in pulses. The charging rate can be controlled by changing the width of pulses. The

interesting feature of this charging method is a short rest period of 20–30 milliseconds

between pulses to stabilize the battery chemical actions [21], [22], [24]. The rest period

enables the chemical reaction to keep pace with the charging process and therefore, can

reduce the gas formation at the electrode surface.

A new pulse-charging method, which is duty-varied voltage pulse-charging strategy was

proposed in [25]. Instead of using the constant pulse width, this method detects and

supplies the suitable charge pulse with varying pulse width to the battery to increase charge speed and charge efficiency.

Meanwhile, negative pulse-charging is a complementary method with pulse-charging. This method applies a very short discharge pulse, during the pulse-charging rest period to depolarize the battery and clear off any gas bubbles built up on the electrode during pulse-charging [21], [22], [26]. Negative pulse-charging is claimed to enhance the overall charging process and prolong the battery lifetime.

In this paper [27], a smart charging method based on fuzzy controller is proposed, in which a charging process is performed with respect to the frequency deviation of grid and state of charge (SOC) of EV battery. In this method, the frequency deviation of grid and current battery SOC of EV are considered as the inputs to fuzzy controller. In the next step, with respect to these inputs and the corresponding membership functions and fuzzy rules, the input power to each EV is determined.

The proposed modified IEEE 39-bus system was divided into three areas. Results of the simulations revealed that, by the proposed method, maximum frequency deviations of areas 1 to 3 was decreased by 36%, 45%, and 22%, respectively, in comparison to dumb charging. Moreover, it was illustrated that, using the proposed method, RMS values of frequency deviations in areas 1 to 3 were reduced by 60%, 59%, and 63%, respectively, compared with the case of using dumb charging.

In another case study, performance of proposed method is compared with an optimized PI controller. The parameters of PI are obtained by imperialist competitive algorithm (ICA)[28]. ICA has been used in various papers owing to its high speed and accuracy in

finding the solutions of optimization problems; theory of this method has been described in detail in [29], [30]. The results of the simulation illustrated a good performance of the proposed method in this case as well so that, by using the proposed method, maximum frequency deviations of areas 1 to 3 were reduced by 31%, 30%, and 32% respectively, when it compared to the optimized PI controller.

Optimal charging management of EVs is crucial for drivers' and power grid operator [31]. In order to maximize drivers' satisfaction and minimize the power grid deterioration, smart charging management (SCM) may be a considerable solution [32]. SCM systems manage EVs charging requirement considering EVs, Charging Stations and power grid together. In addition to that, charge scheduling and charge control are also important and need to be taken under consideration [33].

For that reason, SCM systems use different mathematical models to design an optimization technique for finding the appropriate solution [31]. In this paper [31], a novel double-layer smart charging management algorithm (SCMA) model, is proposed for parking areas. The proposed model of this study, with proper SCMA strategy, not only satisfies driver expectations and increases power grid quality, but also decreases power losses and waste time to reach charging stations. Smart parking areas with the SCMA model offer many benefits to power grid and drivers. For instance, drivers can reach optimal charging point easily by providing desired parameters. Furthermore, less power grid fluctuations, decreased peak power and reduced voltage drop can be obtained. Most of the studies have mainly focused on the controlled and uncontrolled charging strategies for EVs. Uncontrolled charging of EVs may increase the grid problems such as power losses, voltage deviations, and substations overloads [34]. On the other hand, coordinated charging

strategy is proposed to alleviate these problems with different strategies such as time of use (TOU), centralized and distributed control [35], [36].

CHAPTER 3

MODELING AND RESEARCH METHODOLOGY

3.1 Model Selection

There are various techniques reported in literature that can be applied to equivalent-circuit models to extract the battery impedance parameters in real time. For those models requiring a mathematical function to describe the OCV-SOC relationship, a polynomial function, whose order is empirically determined, is employed. Thereafter, a double-EKF is designed to serve as an online cell model states (including SOC) and parameters estimator. The internal resistance or Rint model, as illustrated in the figure 2-4, is comprised of an ideal voltage source VOC to represent the battery's OCV as a function of SOC and a series resistor Rs that describes the internal ohmic losses. This model structure is also linear in parameters and is very 'simple' to implement in real time. However, the model's output equation is only a crude estimate of the battery's actual terminal voltage, which can result in large uncertainties in other model-based battery states (e.g. SOC).
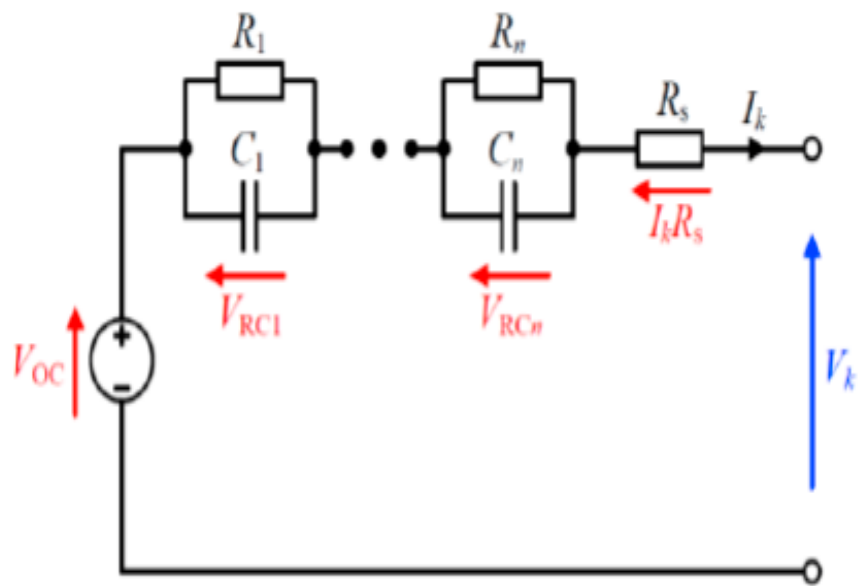
Figure 3-1: Generalized RC Model

The resistor-capacitor (RC) or the Thevenin equivalent-circuit model, as shown in Figure, is a modification of the Rint model. This model is comprised of an ideal voltage source to represent the cell's OCV at partial equilibrium as a function of SOC, a series ohmic-resistance Rs and n number of series-connected parallel RC branches. Depending on the dynamics of the intended application, the number of the RC branches may vary. For most power applications, one RC branch is adequate to describe the long time-constant reactions associated with the diffusion of active species into the electrolyte. Considering applications with faster transients, the short time-constant reactions associated with the charge-transfer and the double-layer effect of the electrodes can be modelled with additional RC branches.

To achieve accurate modeling and state estimation, two key challenges must be addressed, i.e., the hysteresis effect and the long relaxation process. In this thesis, we adopt a second-order electric circuit model coupled with the hysteresis effect as shown in the figure 3-2 , where OCV is the battery open-circuit voltage, and v and i are the battery terminal voltage and current, respectively. Ri represents the battery internal resistance. R1C1 is used to capture the battery short-term relaxation dynamics, while R2C2 for capturing the long-term relaxation process. The overpotentials across these two RC networks are V1 and V2 , respectively. The battery OCV is the battery terminal voltage when the battery internal equilibrium is reached in the absence of load. The battery OCV depends on the battery SOC, temperature, and previous charging/ discharging history, which is referred to as the hysteresis effect and is captured by Vh.
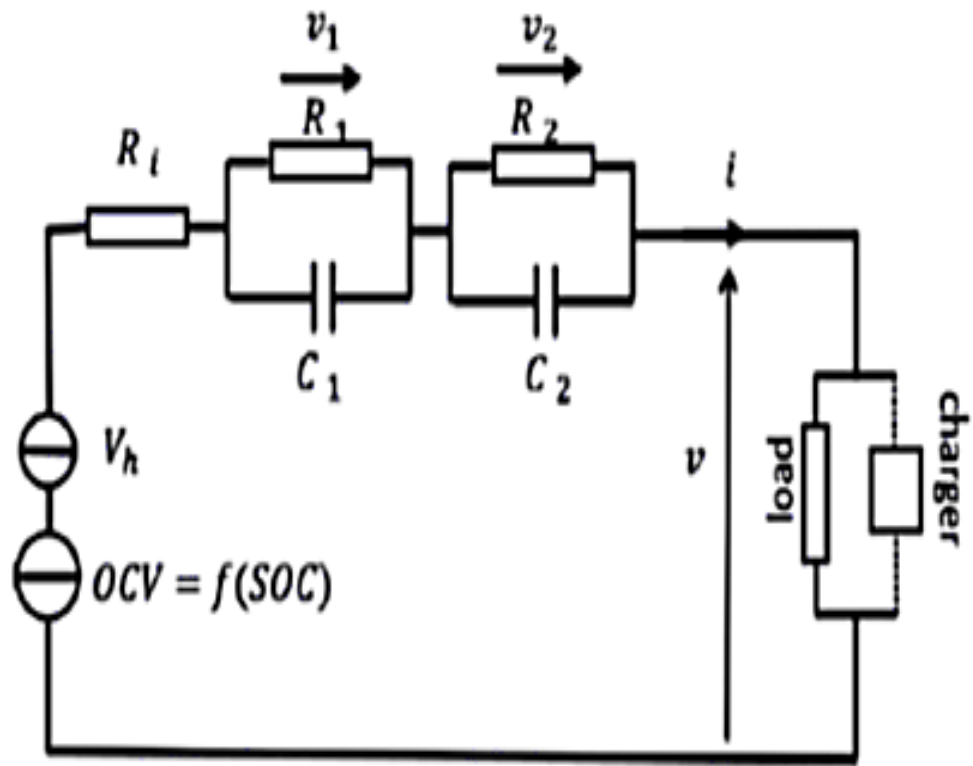
Figure 3-2: Second order RC Model

$$OCV = f(SOC) \tag{3-1}$$

Then the battery SOC could be calculated as follows:

$$SOC(k) = SOC(k-1) + i(k-1) * \frac{\frac{Ts}{3600}}{Cn} \tag{3-2}$$

where Ts is the sampling time in seconds and Cn is the battery nominal capacity in Ampere hour (Ah).

Following the dynamics of an RC network, we have:

$$v_l(k) = a_l * v_l(k-1) + b_l * i(k-1) \tag{3-3}$$

$$\text{Where } a_l = \exp\left(-\frac{\frac{Ts}{R_l}}{C_l}\right) \quad, b_l = R_l * (1 - a_l), \quad l = 1,.$$

The hysteresis effect is represented by the following equation:

$$\begin{aligned}
V_h(k) &= e^{-\gamma*|i(k-1)|} * V_h(k-1) \\
&\quad + (1 - e^{-\gamma*|i(k-1)|}) * \text{sign}(i(k-1)) * M_h \\
&= c_{k-1} * V_h(k-1) + d_{k-1} * M_h
\end{aligned} \tag{3-4}$$

where M_h is the maximum hysteresis value, and γ adjusts the changing rate of V_h.

Combing (3-1 – 3-4), the battery electrical sub model can be described as

$$x_e(k) = A_e(k-1) * x_e(k-1) + B_e(k-1) \qquad \text{(3-5)}$$

where

$$x_e(k) = [\text{soc}(k),\ v_1(k),\ v_2(k),\ V_h(k)]^T$$

and $A_e = \text{diag}([1,\ a_1,\ a_2,\ c_{k-1}])$, $B_e(k-1) = [i(k-1) * T_s/3600/C_n,\ b_1 * i(k-1), b_2 * i(k-1),\ d_{k-1} * M_h]^T$

$$v = \text{OCV} + V_h + R_i * i + v_1 + v_2. \qquad \text{(3-6)}$$

3.2 Double-EKF System Identification

Using the EKF system identification method, the non-linear battery model describing the underlying dynamics of the system is linearized using the Taylor series expansion around the filter's current estimated trajectory. In order to simultaneously estimate both model states and parameters, the double-EKF algorithm is adopted here.

3.2.1 Underlying Theory

With the assumption that the cell terminal current I_k and voltage V_k are the only measurable quantities, the EKF state filter can be designed such that:

$$x_{k+1} = f(x_k, u_k, \theta_k) + w_k$$
$$y_k = h(x_k, u_k, \theta_k) + v_k \tag{3-7}$$
$$w_k \sim N(0, Q^x), \qquad v_k \sim N(0, R^x)$$

where $\mathbf{x}_k \in \mathbb{R}^n$ is a vector containing the model states to be predicted in a minimum variance sense, $\mathbf{\theta}_k \in \mathbb{R}^q$ contains the time-varying model parameters, $\mathbf{u}_k \in \mathbb{R}^p$ is the exogenous model input, $\mathbf{y}_k \in \mathbb{R}^m$ is the output, and $\mathbf{w}_k \in \mathbb{R}^n$ and $\mathbf{v}_k \in \mathbb{R}^m$ are the zero-mean process and measurement noises of covariance $\mathbf{Q}^x$ and $\mathbf{R}^x$ respectively. The nonlinear function $f(\cdot,\cdot,\cdot)$ relates the states estimated at discrete time-step $k-1$ to the states at the current time step k and $h(\cdot,\cdot,\cdot)$ maps the updated states to the measurements at time-step k.

Assuming that the parameters vary slowly over time (i.e. minutes to hours), the weight EKF can be designed to adaptively provide an estimate of the true model parameters. Thus, the state-space model for the weight filter is given as:

$$\theta_{k+1} = \theta_k + r_k$$

$$d_k = h(x_k, u_k, \theta_k) + e_k \tag{3-8}$$

$$r_k \sim N(0, Q^\theta), \qquad e_k \sim N(0, R^\theta)$$

where the dynamics of changes in $\boldsymbol{\theta}_k$ are attributed to a small imaginary white noise $\mathbf{r}_k \in \mathbb{R}^p$ of covariance $\mathbf{Q}^\theta$ that evolves the parameters over time. The output equation $\mathbf{d}_k \in \mathbb{R}^m$ is given as a measurable function of $\boldsymbol{\theta}_k$ and a white noise $\mathbf{e}_k \in \mathbb{R}^m$ of covariance $\mathbf{R}^\theta$ to account for the sensor noise and modelling uncertainties.

Due to the time-variability of the model parameters, it is imperative that the actual input/output cell data (e.g. voltage, current, etc.) convey continual information on the parameters to be estimated. This condition is referred to in system identification literature as the "persistence of excitation" (PE) [57].

In many real-time battery state estimation problems, the load-current profile may not fully satisfy the PE criterion. For those observer-based SOC estimators such as the extended Luenberger observer, sliding mode or adaptive observers, if the PE condition is not sufficiently satisfied, the gains tend to approach infinity and severe divergence occurs [57]. Nevertheless, the EKF algorithm seems to operate well under such conditions without any divergence (e.g. in [39], [62]).

It should be noted that the algorithm is initialized by assuming *a prior* knowledge of the model states and parameters are available. However, in practice, initial system information are usually unknown. Thus, the states and the parameters are set to their best guess values at $k=0$ so that $\hat{\theta}_0^+ = E[\boldsymbol{\theta}_0]$ and $\hat{x}_0^+ = E[\mathbf{x}0]$.

Each time step, the algorithm first updates the state and parameter estimates $\hat{x}_0^-$ and $\hat{\theta}_0^-$ and their error covariance $\boldsymbol{P}_{x,k}^-$ and $\boldsymbol{P}_{\theta,k}^-$ respectively, by propagating them forward in time. Note that for the parameter time-update equation, the new parameter estimate $\hat{\theta}_0^-$ is equal to the previous estimate $\hat{\theta}_{k-1}^+$ with an increase in its uncertainty due to the presence of the white process noise $\mathbf{r}_k$.

After a measurement has been taken at time step k, both filters take this measurement into consideration to update the state and parameter estimates $\hat{x}_k^+$ and $\hat{\theta}_k^+$ and their corresponding uncertainties as $\boldsymbol{P}_{x,k}^+$ and $\boldsymbol{P}_{\theta,k}^+$respectively. The measurement-update error covariance matrices $\boldsymbol{P}_{x,k}^+$ and $\boldsymbol{P}_{\theta,k}^+$ are given in their Joseph forms to ensure a numerically robust algorithm.

It is noted that for the weight filter's measurement-update equations, the total-differential $\mathbf{H}_k^\theta$ of the model output equation $h(\cdot,\cdot,\cdot)$ with respect to parameters $\boldsymbol{\theta}_k$ is required. Therefore, by decomposing the total-derivative into partial-derivatives, $\mathbf{H}_k^\theta$ is computed recursively as the following set of equations:

$$
\mathbf{H}_k^\theta = \left.\frac{dh(\hat{x}_k^-, u_k, \theta_k)}{d\theta_k}\right|_{\theta_k = \hat{\theta}_k^-}
$$

$$
\frac{dh(\hat{x}_k^-, u_k, \hat{\theta}_k^-)}{d\hat{\theta}_k^-} = \frac{\partial h(\hat{x}_k^-, u_k, \hat{\theta}_k^-)}{\partial \hat{\theta}_k^-} + \frac{\partial h(\hat{x}_k^-, u_k, \hat{\theta}_k^-)}{\partial \hat{x}_k^-} \cdot \frac{d\hat{x}_k^-}{d\hat{\theta}_k^-}
$$

$$
\frac{d\hat{x}_k^-}{d\hat{\theta}_k^-} = \frac{\partial f(\hat{x}_{k-1}^+, u_{k-1}, \hat{\theta}_k^-)}{\partial \hat{\theta}_k^-} + \frac{\partial f(\hat{x}_{k-1}^+, u_{k-1}, \hat{\theta}_k^-)}{\partial \hat{x}_{k-1}^+} \cdot \frac{d\hat{x}_{k-1}^+}{d\hat{\theta}_k^-}
$$

$$
\frac{d\hat{x}_{k-1}^+}{d\hat{\theta}_k^-} = \frac{d\hat{x}_{k-1}^-}{d\hat{\theta}_{k-1}^+} - \mathbf{L}_{k-1}^x \frac{dh(\hat{x}_{k-1}^-, u_{k-1}, \hat{\theta}_{k-1}^+)}{d\hat{\theta}_{k-1}^+}
$$

(3-9)

L_{k-1}^x is weakly related to the parameter estimates $\boldsymbol{\theta}_k$, hence, it can be safely neglected in (3-9) to improve the computation efficiency of the weight filter. Furthermore, $d\hat{x}_{k-1}^+/d\hat{\theta}_k^-$ is set to zero at $k=0$ and the three total-derivatives are updated recursively.

To summarize all the double-EKF algorithm steps for battery model state and parameters estimation, below are the required equations.

- Initialization:

$$\hat{\theta}_0^+ = E[\theta_0], \qquad P_{x,0}^+ = E\left[(\theta - \hat{\theta}_0^+)(\theta - \hat{\theta}_0^+)^T\right]$$

$$\hat{x}_0^+ = E[x_0], \qquad P_{x,0}^+ = E\left[(x - \hat{x}_k^+)(x - \hat{x}_k^+)^T\right] \tag{3-10}$$

- Time-update equations for state filter:

$$\hat{x}_k^- = f\left(\hat{x}_{k-1}^+, u_{k-1}, \hat{\theta}_k^-\right)$$

$$P_{x,k}^- = F_{k-1} P_{x,k}^+ F_{k-1}^T + Q_k^x \tag{3-11}$$

- Time-update equations for weight filter:

$$\hat{\theta}_k^- = \hat{\theta}_{k-1}^+$$

$$P_{\theta,k}^- = P_{\theta,k-1}^+ + Q_k^\theta \tag{3-12}$$

- Measurement-update equations for state filter:

$$L_k^x = P_{x,k}^- (H_k^x)^T \left[H_k^x P_{x,k}^-(H_k^x)^T + R_k^x\right]^{-1}$$

$$\hat{x}_k^+ = \hat{x}_k^- + L_k^x \left[y_k - h\left(\hat{x}_k^-, u_k, \hat{\theta}_k^-\right)\right] \tag{3-13}$$

$$P_{x,k}^+ = (I - L_k^x H_k^x) P_{x,k}^- (I - L_k^x H_k^x)^T + L_k^x R_k^x (L_k^x)^T$$

- Measurement-update equations for weight filter:

$$\mathbf{L}_k^\theta = \boldsymbol{P}_{\theta,k}^- \left(\boldsymbol{H}_k^\theta\right)^T \left[\boldsymbol{H}_k^\theta \, \boldsymbol{P}_{\theta,k}^-\left(\boldsymbol{H}_k^\theta\right)^T + \boldsymbol{R}_k^\theta\right]^{-1}$$

$$\hat{\theta}_k^+ = \hat{\theta}_k^- + \mathbf{L}_k^\theta \left[\mathbf{d}_k - h\left(\hat{x}_k^-, u_k, \hat{\theta}_k^-\right)\right] \tag{3-14}$$

$$\boldsymbol{P}_{\theta,k}^+ = \left(I - \mathbf{L}_k^\theta \, \boldsymbol{H}_k^\theta\right) \boldsymbol{P}_{\theta,k}^- \left(I - \mathbf{L}_k^\theta \, \boldsymbol{H}_k^\theta\right)^T + \mathbf{L}_k^\theta \boldsymbol{R}_k^\theta \left(\mathbf{L}_k^\theta\right)^T$$

Where,

$$\boldsymbol{F}_{k-1} = \left.\frac{\partial f\left(x_{k-1}, u_{k-1}, \hat{\theta}_k^-\right)}{\partial x_{k-1}}\right|_{x_{k-1}=\hat{x}_{k-1}^+},$$

$$\boldsymbol{H}_k^x = \left.\frac{\partial h\left(x_k, u_k, \hat{\theta}_k^-\right)}{\partial x_k}\right|_{x_k=\hat{x}_k^-}, \tag{3-15}$$

$$\mathbf{H}_k^\theta = \left.\frac{dh(\hat{x}_k^-, u_k, \theta_k)}{d\theta_k}\right|_{\theta_k=\hat{\theta}_k^-}.$$

3.2.2 Estimation of EKF Noise Statistics

The convergence and tracking performance of any KF-based system identification technique is largely dependent on the process and measurement noise statistics initialized at time-step $k=0$. In most researches conducted on battery system identification using KF-based algorithms, these two statistical parameters are either tuned manually, which can be a tedious task, or set by experience. In this thesis, the expectation maximization (EM) algorithm is employed to provide an iterative maximum-likelihood estimate for the filters' process and measurement noise statistical parameters (i.e. $\mathbf{Q}^x$ and $\mathbf{R}^x$ for the state EKF and $\mathbf{Q}_\theta$ and $\mathbf{R}_\theta$ for the weight EKF).

In general, for a nonlinear joint-optimization problem, where both model states and parameters are unknown, the EM algorithm performs a joint maximization of the conditional probability density functions for both the states vector $\mathbf{x}_k$ and the parameters vector $\boldsymbol{\theta}_k$. The resulting algorithm can, thus, be used as an alternative to the double-EKF estimator for online BES identification problems. However, this comes at an increased computational cost, which is a subject of study in its own merits.

3.2.2.1 Estimation of process noise covariance Q

For a measurement vector, $\mathbf{y}_N$, of sample size N, the covariance $\mathbf{Q}$ of the zero-mean white process noise $\mathbf{w}_k \sim N(0,\mathbf{Q})$ can be defined as:

$$Q = \frac{1}{N}\sum_{k=1}^{N} E[w_k w_k^T | y_n] \qquad (3\text{-}16)$$

Then, considering the state-space equations given in (3-7), the process noise, $\mathbf{w}_k$, for a double-EKF can be approximated using the first-order Taylor series expansion leading to:

$$w_k \approx x_k - f\left(x_{k-1|N}, u_{k-1|N}, \theta_{k-1|N}\right) - \mathbf{F}_{k-1|N}\tilde{x}_{k-1|N} \tag{3-17}$$

where $\mathbf{F}_{k-1|N}$ is the Jacobian of the nonlinear function $f(\cdot)$ and $\tilde{\mathbf{x}}_{k-1|N} = \mathbf{x}_{k-1} - \mathbf{x}_{k-1|N}$.

Subsequently, using (3-17), the outer product of $\mathbf{w}_k$, as required in (3-16), can be expressed as:

$$
\begin{aligned}
w_k w_k^T =\ & x_k x_k^T - x_k f\left(x_{k-1|N}, u_{k-1|N}, \theta_{k-1|N}\right)^T - f\left(x_{k-1|N}, u_{k-1|N}, \theta_{k-1|N}\right)x_k^T \\
& + f\left(x_{k-1|N}, u_{k-1|N}, \theta_{k-1|N}\right)f\left(x_{k-1|N}, u_{k-1|N}, \theta_{k-1|N}\right)^T \\
& - x_k \tilde{x}^T{}_{k-1|N}\, \mathbf{F}^T{}_{k-1|N} + f\left(x_{k-1|N}, u_{k-1|N}, \theta_{k-1|N}\right)\tilde{x}^T{}_{k-1|N}\, \mathbf{F}^T{}_{k-1|N} \\
& - \mathbf{F}_{k-1|N}\tilde{x}_{k-1|N}x_k^T + \mathbf{F}_{k-1|N}\tilde{x}_{k-1|N}f\left(x_{k-1|N}, u_{k-1|N}, \theta_{k-1|N}\right)^T \\
& + \mathbf{F}_{k-1|N}\tilde{x}_{k-1|N}\tilde{x}^T{}_{k-1|N}\, \mathbf{F}^T{}_{k-1|N}\ .
\end{aligned}
\tag{3-18}
$$

The conditional expectation for a state vector $\mathbf{x}_k$ to be estimated, given measurements of up to and including $\mathbf{y}_N$ are available, can be expressed as:

$$
\begin{aligned}
E[x_k x_k^T | y_N] &= x_{k|N} x_{k|N}^T + \mathbf{P}_{k|N} \\
E[x_k x_{k-1}^T | y_N] &= x_{k|N} x_{k-1|N}^T + \mathbf{P}_{k,k-1|N}
\end{aligned}
\tag{3-19}
$$

where the lagged covariance $\mathbf{P}_{k,k-1|N}$ is defined by:

$$
\begin{aligned}
\mathbf{P}_{k,k-1|N} &= E\left[\left(x_k - x_{k|N}\right)\left(x_{k-1} - x_{k-1|N}\right)^T\right] \\
&= \mathbf{P}_{k|k}\mathbf{L}_{k-1|N}^T + \mathbf{L}_{k|N}\left(\mathbf{P}_{k+1,k|N} - \mathbf{F}_k\mathbf{P}_{k|k}\right)\mathbf{L}_{k-1|N}^T
\end{aligned}
\tag{3-20}
$$

Subsequently, by rearranging equations (3-18) to (3-20), the conditional expectation defined in (3.16) can be given as :

$$Q = \frac{1}{N} \sum_{k=1}^{N} (w_{k|N} w_{k|N}^T + P_{k|N} + F_{k-1|N} P_{k-1|N} F^T{}_{k-1|N} - P_{k,k-1|N} F^T{}_{k-1|N}$$

$$- P^T{}_{k,k-1|N} F_{k-1|N}) \tag{3-21}$$

where $\mathbf{w}_{k|N} = \mathbf{x}_{k|N} - f(\mathbf{x}_{k-1|N}, \mathbf{u}_{k-1}, \boldsymbol{\theta}_{k-1|N})$.

3.2.2.2 Estimation of measurement noise covariance R

Similar to **Q** estimation, for the same sample of size N, the measurement noise covariance **R** can be defined as:

$$R = \frac{1}{N} \sum_{k=1}^{N} E[v_k v_k^T | \mathbf{y}_N] \tag{3-22}$$

where $\mathbf{v}_k \sim N(0, \mathbf{R})$ is the zero-mean white-color noise introduced by the current and voltage sensors. Then, using $\mathbf{v}_k = \mathbf{y}_k - h(\mathbf{x}_k, \mathbf{u}_k, \boldsymbol{\theta}_k)$ as per (3-7), the measurement noise, $\mathbf{v}_k$ can be approximated using the first-order Taylor series expansion and given as:

$$v_k \approx y_k - h(x_{k|N}, u_{k|N}, \theta_{k|N}) - H_{k|N} \tilde{x}_{k|N} \tag{3-23}$$

where $\mathbf{H}_{k|N}$ is the Jacobian of the nonlinear function $h(\cdot)$ and $\tilde{\mathbf{x}}_{k|N} = \mathbf{x}_k - \mathbf{x}_{k|N}$.

Subsequently, using (3-24), the outer product of $\mathbf{v}_k$, and following the procedure as in

producing the Q in the previous section, equation (3-22) could be written as :

$$R = \frac{1}{N}\sum_{k=1}^{N}(v_{k|N}v_{k|N}^{T} + H_{k|N}P_{k|N}H^{T}{}_{k|N}) \tag{3-24}$$

where $\mathbf{v}_{k|N}=\mathbf{y}_k-h(\mathbf{x}_{k|N},\mathbf{u}_k,\boldsymbol{\theta}_{k|N})$.

3.2.2.3 Initialized $\boldsymbol{Q}$ and $\boldsymbol{R}$ Values

using a sample size of $N=1000$, equations (3-21) and (3-24) were applied to the double-EKF

algorithm to estimate the state and weight filters' noise covariance. The chosen sample size

implies that for the sampling period of $\Delta t=100$ ms used here, there will be 100 seconds of

data in every window. This allows for those model parameters with slow transients to be

assumed steady over the period of 100 seconds. Finally, the process and measurement noise

covariance for EKFs are initialized as per (3-25).

$$\boldsymbol{Q}_0^x = diag_n\{1\times 10^{-6}\}, \quad \boldsymbol{P}_{\tilde{x},0}^+ = diag_n\{10\}, \quad \boldsymbol{R}_0^x = diag_m\{10\}$$
$$\tag{3-25}$$
$$\boldsymbol{Q}_0^\theta = diag_q\{1\times 10^{-8}\}, \quad \boldsymbol{P}_{\tilde{\theta},0}^+ = diag_q\{10\}, \quad \boldsymbol{R}_0^\theta = diag_m\{10\}$$

where diag$\{\cdot\}$ is a diagonal matrix of size $n\times n$ for $\boldsymbol{Q}_0^x$ and $\boldsymbol{P}_{\tilde{x},0}^+$, $q\times q$ for $\boldsymbol{Q}_0^\theta$ and $\boldsymbol{P}_{\tilde{\theta},0}^+$, and

$m\times m$ for $\boldsymbol{R}_0^x$ and $\boldsymbol{R}_0^\theta$ matrices, respectively. Note that the error covariance matrices $\boldsymbol{P}_{\tilde{x},0}^+$

and $\boldsymbol{P}_{\tilde{\theta},0}^+$ are set to a large value at the initialization time-step $k=0$ in order to account for

any uncertainties in the filters' initial conditions.

3.3   Double-EKF Performance Under Incorrect Initial Conditions

In order to initialize the double-EKF algorithm for the real-time estimation of both battery states and parameters, a sufficient knowledge of the unknown parameters to be estimated is often a necessity. In case of erroneous initial battery states, such as SOC, depending on the dynamic structure of the employed battery model, convergence of the battery states is achievable. Although, the rate of convergence can vary for different conditions. Difficulty arises when there exists a large uncertainty in the initial model parameters, i.e. in $\theta_k=\{R\mathrm{s},R1,C1,R2,C2\}$. This is due to the fact that, although the 2-RC network model representation of the battery dynamics is linear in states, the relationship between the incorporated parameters is heavily nonlinear. As a result, convergence towards the expected parameter values might not be possible under erroneous initial parameter settings.

Furthermore, due to the time-variability of the modelled battery parameters, the input/output signal (i.e. terminal current/voltage signal) must be persistently exciting at all times. This pre-condition is a necessity for any online parameter identification technique to be able to properly reveal the contents of the battery's dynamics, whilst running in real time. However, in many real battery systems (e.g. in EVs), the current signal may not be sufficiently exciting at all times (e.g. during open-circuit or static charge/discharge periods). In practice, the double-EKF algorithm, seems to operate well without any divergence [57].

This is true, if and only if, a sufficient knowledge of the model parameters is available at the initialization step. Otherwise, convergence might never be achieved; even though the error covariance matrices for the weight filter in the double-EKF could be approaching zero. In most double-EKF-based BMS algorithms, the battery model parameters are often initialized/calibrated through an offline process, which can be impractical in intermittent BESS applications. Therefore, in most cases, the initial parameters are either set arbitrarily based on experience, or they are approximated by using the information provided in the manufacturer's datasheet. Hence, in this section, the performance of the double-EKF algorithm with respect to erroneous initial conditions is investigated.

3.3.1　Formulation of State-Space Equations

Considering the single RC branch, the transient voltage-drop across V_{RC} across the resistor R and the capacitor C with respect to input current I can be realized. According to Kirchhoff's current law, the amount of current flowing into the branch must be equal to that leaving it. Thus:

$$I = \frac{V_{RC}}{R} + C\frac{dV_{RC}}{dt} \tag{3-26}$$

Rearranging equation (3-26) leads to a first-order differential equation which can be solved by using the technique of separable variables, resulting the following formula:

$$V_{RC}(t_1) = [V_{RC}(t_0) - IR]e^{\frac{-\Delta t}{RC}} + IR \tag{3-27}$$

where $V_{RC}(t_0)$ is the initial voltage across the RC branch at discrete time-step k, $V_{RC}(t_1)$ is the voltage across the same branch at discrete time-step $k+1$ and Δt is the sampling period; note that $t_1 > t_0$. Subsequently, an expression for the transient voltage-drop across each branch of the 2-RC battery model could be deduced in discrete form and given as:

$$V_{RC1_{k+1}} = \left[V_{RC1_k} - I_k R_1 \right] e^{\frac{-\Delta t}{R_1 C_1}} + I_k R_1$$

$$V_{RC1_{k+2}} = \left[V_{RC2_k} - I_k R_2 \right] e^{\frac{-\Delta t}{R_2 C_2}} + I_k R_2$$

(3-28)

Finally, by applying the superposition theorem to the 2-RC equivalent-circuit model, the state-space equations in discrete time required for the double-EKF algorithm can be realized and expressed as:

$$f(\cdot) = \begin{bmatrix} x_1 \\ x_2 \\ x_3 \end{bmatrix} = \begin{bmatrix} SOC_{k+1} \\ V_{RC1_{k+1}} \\ V_{RC2_{k+2}} \end{bmatrix}$$

$$= \begin{bmatrix} 1 & 0 & 0 \\ 0 & e^{\frac{-\Delta t}{\tau_1}} & 0 \\ 0 & 0 & e^{\frac{-\Delta t}{\tau_2}} \end{bmatrix} \begin{bmatrix} SOC_k \\ V_{RC1_k} \\ V_{RC2_k} \end{bmatrix}$$

(3-29)

$$+ \begin{bmatrix} \dfrac{-\eta \Delta t}{Q_{actual}} & 0 & 0 \\ 0 & R_1 \left(1 - e^{\frac{-\Delta t}{\tau_1}} \right) & 0 \\ 0 & 0 & R_2 \left(1 - e^{\frac{-\Delta t}{\tau_2}} \right) \end{bmatrix} I_k$$

$$\theta_k = [R_s, R_1, \tau_1, R_2, \tau_2]^T$$

$$h(\cdot) = V_k = V_{OC}(SOC_k) - V_{RC1_k} - V_{RC2_k} - I_k R_s$$

where $f(\cdot)$ and $h(\cdot)$ are the nonlinear state transition and observation models respectively and $\tau_1 = R_1 C_1$ and $\tau_2 = R_2 C_2$ are long and short transient time-constants respectively, and Q_{actual} was realized earlier from equation (2-1), which represent battery's coulombic efficiency . Assuming the state-filter gain L_k^x is weakly related to the parameters vector θ_k, the Jacobian matrices required for the recursive double-EKF algorithm presented in 3.2.1 previously, could be computed as:

$$F_{k-1} = \left.\frac{\partial f(\cdot)}{\partial x_k}\right|_{x_k = \hat{x}_{k-1}^+} = \begin{bmatrix} 1 & 0 & 0 \\ 0 & e^{\frac{-\Delta t}{\tau_1}} & 0 \\ 0 & 0 & e^{\frac{-\Delta t}{\tau_2}} \end{bmatrix} \tag{3-30}$$

$$\left.\begin{array}{l} \mathbf{H}_k^\theta = \left.\frac{dh(\cdot)}{d\theta_k}\right|_{\theta_k = \hat{\theta}_k^-} = \frac{\partial h(\cdot)}{\partial \hat{\theta}_k^-} + \frac{\partial h(\cdot)}{\partial \hat{x}_k^-} \cdot \frac{d\hat{x}_k^-}{d\hat{\theta}_k^-} \\[4mm] \frac{d\hat{x}_k^-}{d\hat{\theta}_k^-} = \frac{\partial f(\cdot)}{\partial \hat{\theta}_k^-} + \frac{\partial f(\cdot)}{\partial \hat{x}_{k-1}^+} \cdot \frac{d\hat{x}_{k-1}^+}{d\hat{\theta}_k^-} \\[4mm] \frac{\partial h(\cdot)}{\partial \hat{x}_k^-} = \begin{bmatrix} -I_{k-1} & 0 & 0 & 0 & 0 \end{bmatrix} \\[4mm] \frac{d\hat{x}_k^-}{d\hat{\theta}_k^-} = \begin{bmatrix} 0 & 0 & 0 & 0 & 0 \\ 0 & a_{2,2} & a_{2,3} & 0 & 0 \\ 0 & 0 & 0 & a_{3,4} & a_{3,5} \end{bmatrix} \end{array}\right\} \tag{3-31}$$

where:

$$a_{2,2} = -I_{k-1} \cdot (\exp(\Delta t/\tau_1^2) - 1)$$

$$a_{2,3} = (\Delta t/\tau_1^2) \cdot (\hat{x}_{2,k}^- - I_{k-1}R_1)\exp(\Delta t/\tau_1)$$

$$a_{3,4} = -I_{k-1} \cdot (\exp(\Delta t/\tau_2^2) - 1)$$

$$a_{3,5} = (\Delta t/\tau_2^2) \cdot (\hat{x}_{3,k}^- - I_{k-1}R_2)\exp(\Delta t/\tau_2)$$

CHAPTER 4

RESULTS AND DISCUSSION

This chapter highlights the result of applying the proposed methods and discusses its effectiveness in improving the state of charge estimation and the overall charging performance. A set of case-studies is considered to verify the robustness of the proposed controllers under different scenarios.

The results confirm the efficacy of the proposed approaches to greatly the SOC estimation, hence the general charging scheme.

4.1   Validate the Proposed Model

As it has been discussed earlier in section 2.2.1 , different technique of modeling the battery have been mention. The one that is proposed to work with in this thesis is the second order RC model, since it shows its robustness throughout the literature. However, to verify that, at first, a case study had been done, to estimate the voltage of the battery using two different models, which are the Rint model, and the second order RC model.

As it shows in Figure 4-2, the RC model is almost identical to the reference, with a small percentage of error that reaches almost 0.8% , at the beginning of the run time, and that's due to the fact that, the DEKF needed a little bit of a time to cope with the system to identify the measurements.
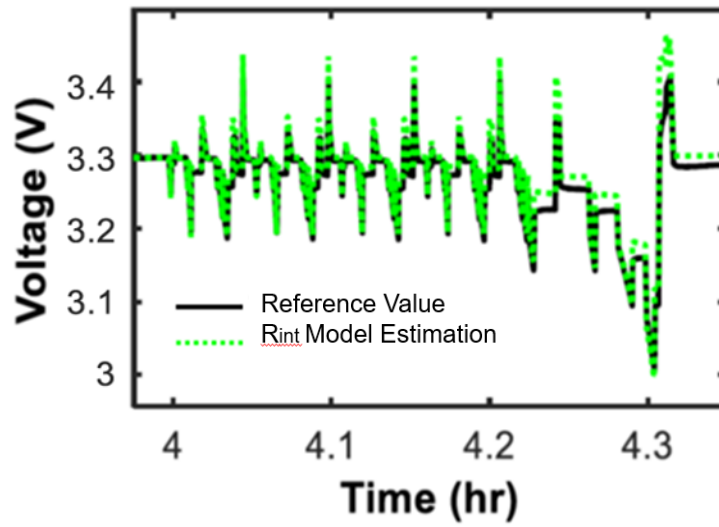
Figure 4-1: Voltage estimation using the Rint Model
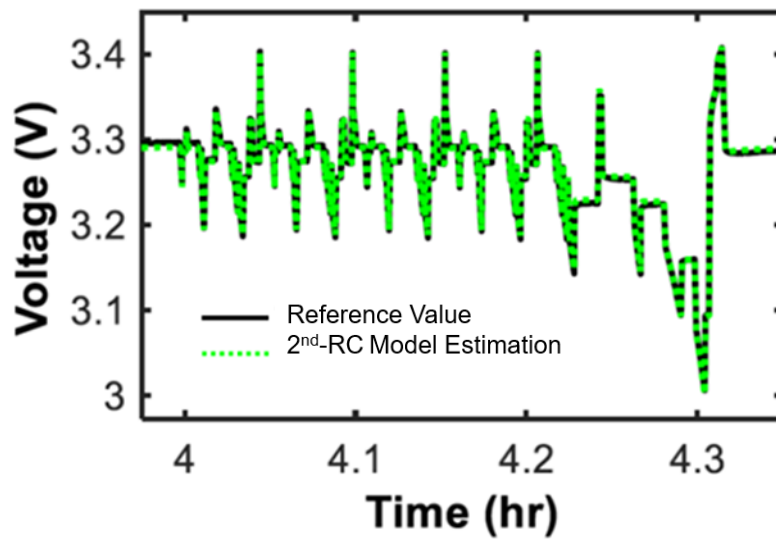
Figure 4-2: Voltage estimation using the Second order RC Model

While on the other hand, the Rint model, on Figure 4-1 have shown a lot of "spicks", and overshooting throughout the procedure, with a maximum of error of around 7%, in addition

53

to some other differences between 1.5-5 %. Form observing the graph, it's noticeable that it shows some acceptable estimation. However, generally, and for more accurate results in the remaining of the research, the RC model has shown a very good estimation for the long period of the procedure.

The second examination for these two models was the state of charge estimation process. Even though on the long sight, and because of the DEKF robustness, the output results show some good estimation for the both models, as it illustrated in Figure 4-3.
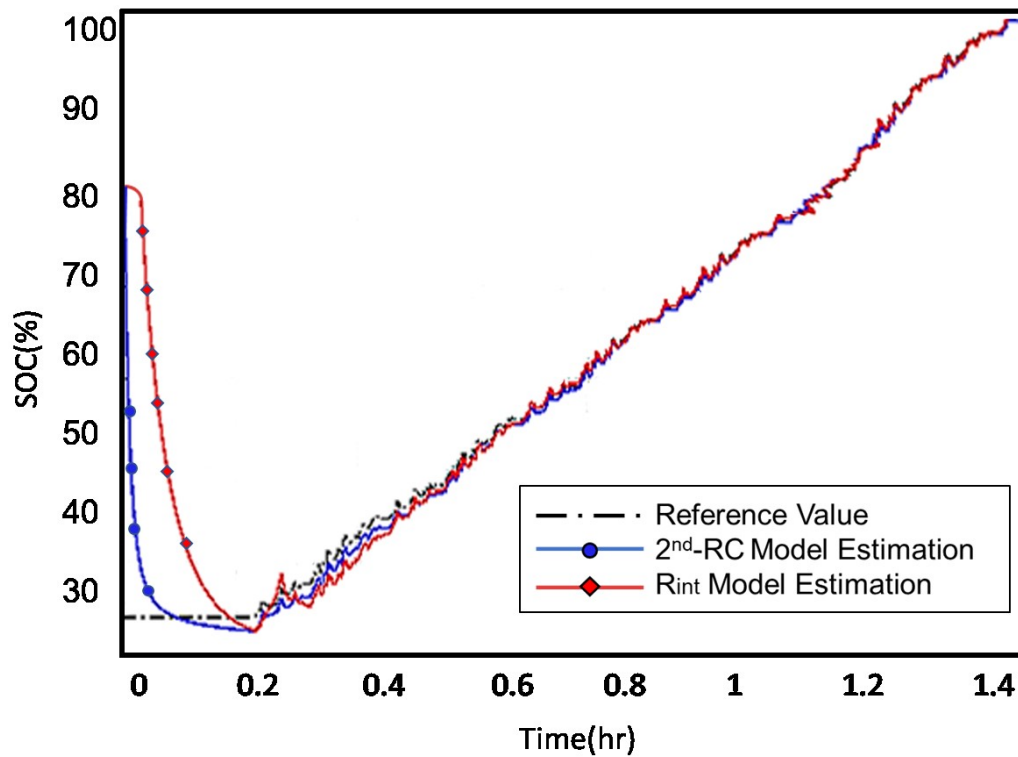
Figure 4-3: SOC with initialization at 80% for both Second order RC and Rint Models

However, what gave the RC model the superiority in this experiment is its quick response to follow and estimate the desired SOC. To examine that, the system was the SOC state was intentionally initialized to 80% to verify the filter's convergence and rapidly it could get the real value. It could be notice that, while the proposed RC model took almost 5 minutes to start following the reference value, the Rint model took almost 3 times that time, to start its tracking at around 14 minutes form the initialization of the examination. This reduction in time by around 60%, have shown that the proposed model is work with more efficiency than the conventional one.

For the accuracy of the estimation, and as predicted, the second order RC had shown its precision with a maximum percentage of error of around only 6%. While in contrast, that maximum value of error in the Rint model had reached almost douple that number at around 13%. The exact values along with the Average percentage of error are shown in table 4-1.

<div align="center">

Table 4-1: Percentage of error for both models

Model	Average Error %	Maximum Error %
Rint	12.3	13.8
Two-RC model	2.01	6.37

</div>

4.2   Model Parameter Identification

Identifying the second order RC parameters is one of the main feature of this proposed battery management system. The resistors, which are the main concern since they are the main source of losing power, and making the measurement not accurate is it supposed to be will be our main concern, Rs, R_1 and R_2, along with the capacitances C_1 and C_2.

The proposed DEKF was used to identify these values throughout different values of the state of charge of the battery. In order to compare the efficiency and the strength of the DEKF, the identification first was done using the ordinary Kalman Filter. Even though the KF showed its well-known strength, but overall, the DEKF had shown is robustness and accuracy, especially in estimating the resistance values, with maximum percentage of error in the R_2, with almost 1.3 % , while in the KF the percentage of error for the same component reached almost more than 2 times that value.

The noticeable thing about the overall result is the estimation of the capacitors, specifically the C_2, which had a percentage of error of around 24% when using the KF, while this value reached near 20% when the DEKF was used. The reason for the noticeable divergence may came from the nature of the representation of the capacitor in this model, along with the differential equation representation for the capacitor. Yet, this value could be acceptable, since throughout the literature, the focus is always around the Resistance values while the capacitors are being ignored. And this could be an individual research topic in the future, since the understanding of the capacitors in general and super capacitors in particular is one of the hot topics in the research area in the upcoming decade, hence more attention and study on the capacitors will be performed

Figure 4-4 below show the produced results. While table 4-2 present the overall percentage of error for all the component using the KF and DEKF.
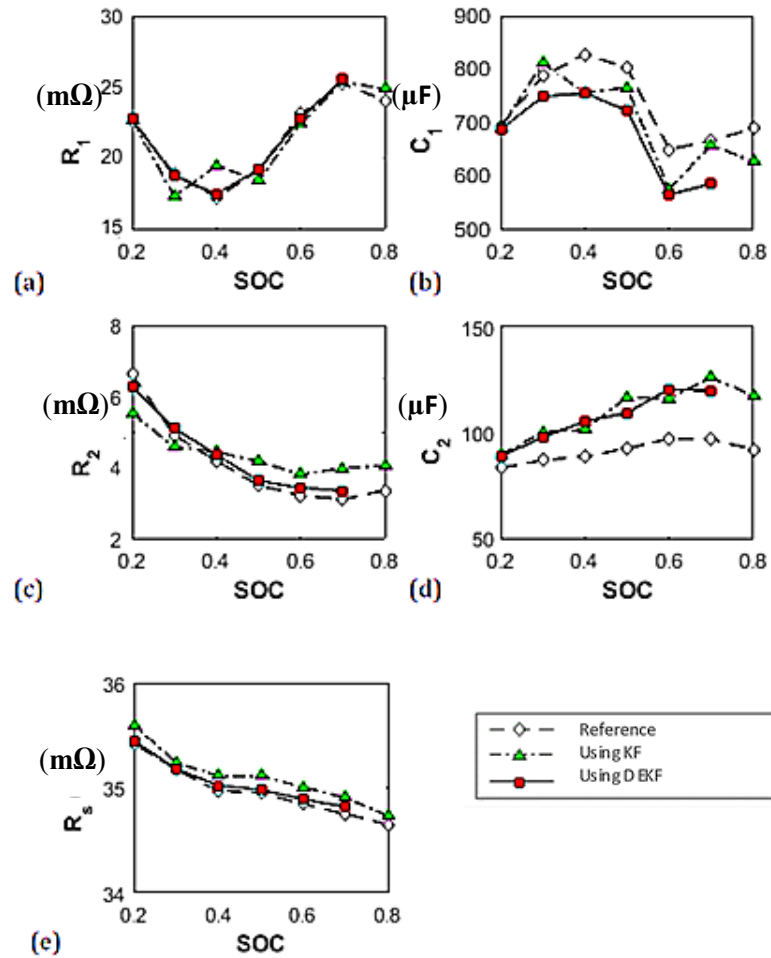

Figure 4-4: Parameter Identification for the Second Order RC Model using KF and DEKF

Table 4-2: Percentage of error in Estimating the Second Order RC Parameters

Mean Absolute Error (MAE%)					
Method of Estimation	Parameters				
	Rs	R_1	C_1	R_2	C_2
KF	0.387	0.142	5.36	3.61	24.03
DEKF	0.129	0.123	8.26	1.32	20.42

In order to validate the proposed estimation method, an additional examination was done, in which an injected noise was added to the measurement in order to test the strength of the DEKF and how the estimated values will come. And again, it was compared to the ordinary KF.

The overall results have shown the robustness and the good estimation of the DEKF with the addition of the noise when compared to KF. And as expected, the maximum error in the estimated resistors was as previous in the R_2 , with 4.76 % , and that's for the DEKF, while for the same parameter in the KF the percentage of error had reached almost double the that in the DKEF, with almost 7.5%.

The best estimation was record in the R_s value with less than 0.5%, and this great accuracy for this parameter may come from the fact that its estimation equations is not as complicated as the rest of the parameters. Moreover, the overall highest percentage of error was recorded at the C_2, which could be related to the nature of the capacitors when it uses a mathematical representation in the system.

The results for all parameters are shown in figure 4-5 , while the overall percentage of error for the second case are shown in table 4-3.
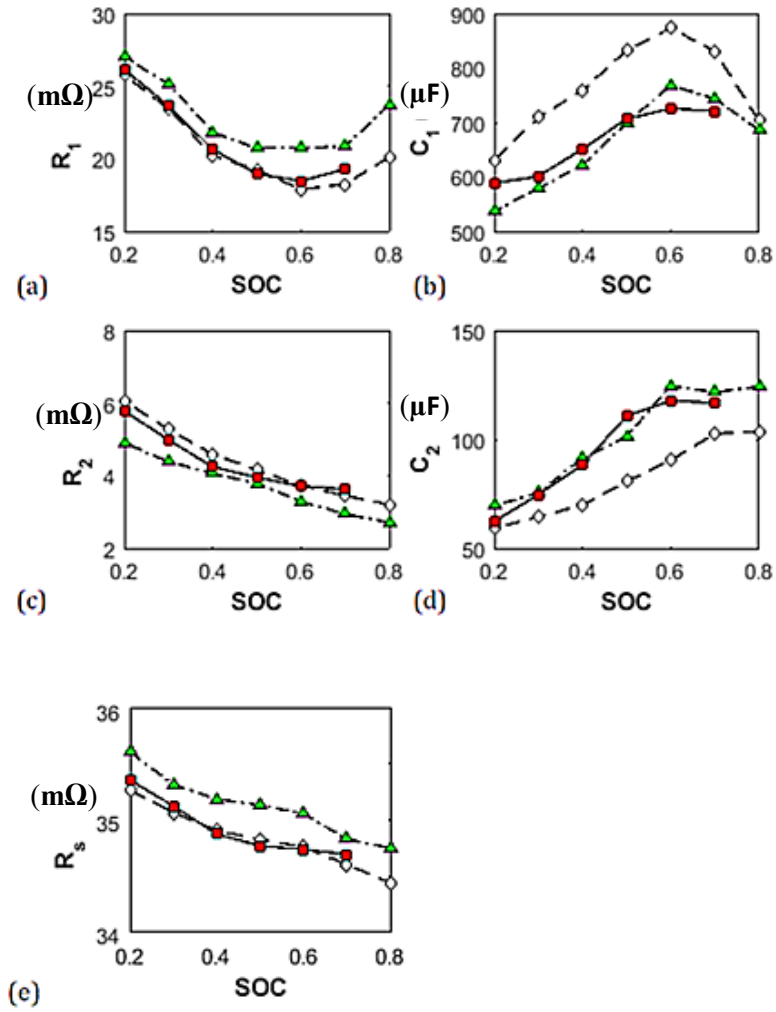
Figure 4-5: Parameter Identification for the Second Order RC Model using KF and DEKF with the addition of Noise

Table 4-3: Percentage of error in Estimating the Second Order RC Parameters with the addition of Noise

Mean Absolute Error (MAE%)					
Method of Estimation	Parameters				
	Rs	R_1	C_1	R_2	C_2
KF	2.04	8.42	13.2	7.48	24.94
DEKF	0.34	3.09	12.35	4.76	21.25

4.3   Real Time Digital Simulator (RTDS)

This section illustrates an experimental validation of the proposed battery management system with the enhancement of the DEKF design on RTDS (real time digital simulator). It has a significant feature over traditional simulation software such as MATLAB and PSCAD/EMTDC which is "online hard real-time simulation". This allows RTDS to be interfaced with power system hardware equipment, such as commercial relay and external controller in real-time. Compared with conventional simulation packages, RTDS is computationally faster, time-saving and more accurate.

To test the effectiveness of the proposed control strategy, experimental work has been performed in a hardware platform. The experimental setup is shown in figure 4-6 the proposed estimation and control method is built in d-SPACE/DS1103, while RTDS is used to simulate the rest of the plant. The digital signals are transmitting back and forth between RTDS-RACK and d-SPACE board through their input/output ports. The dSPACE library should be-first- interfaced with MATLAB/SIMULAINK library, then certain blocks can be used for signal sending and receiving from DS1103 board. After implementing the controller in MATLAB/SIMULAINK, it was downloaded to the d-SPACE processor using (***Build Model***) command and then the controller is ready to be used.
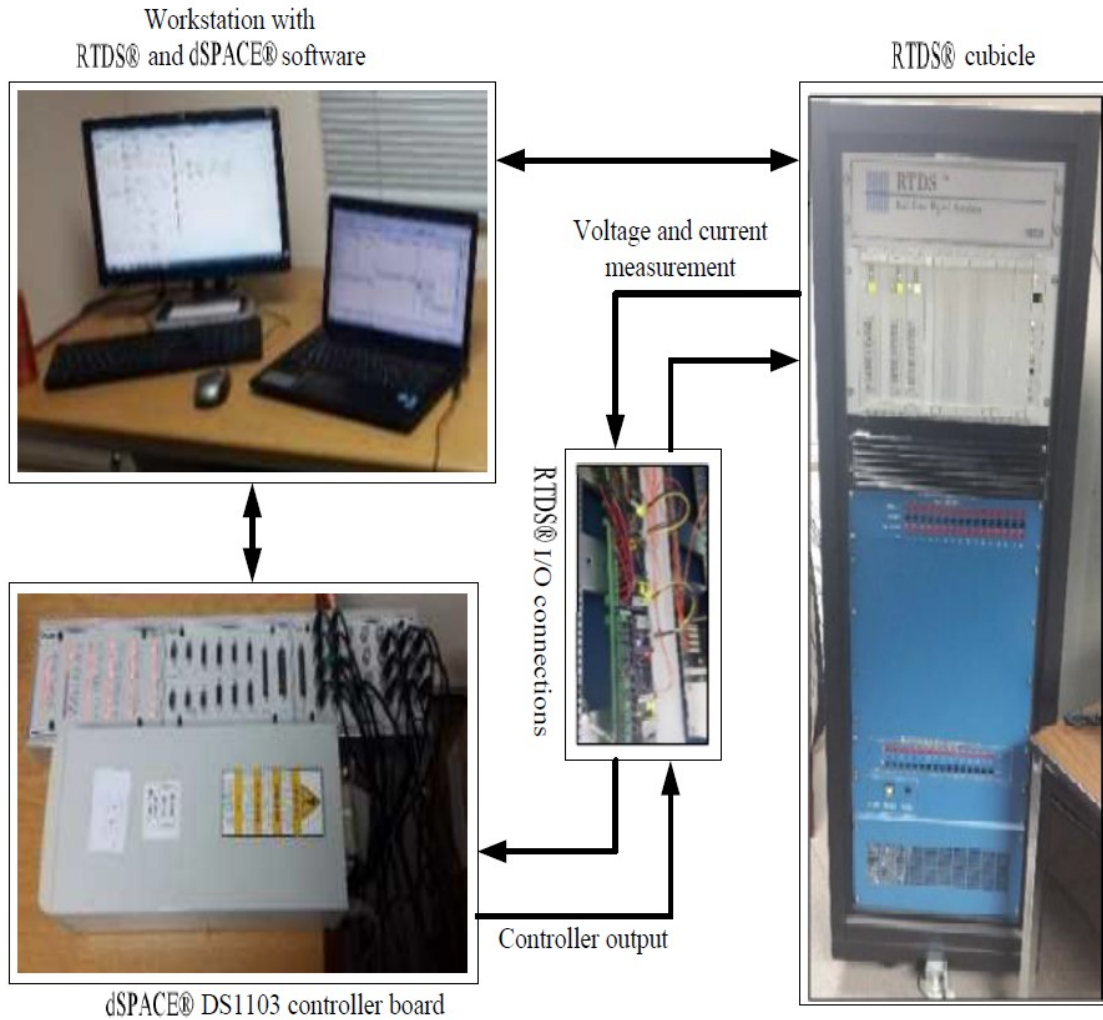
Figure 4-6. Experimental setup

In this part, the two-main case study were implemented, which are the SOC Estimation process, and the main objective of the BMS which is the charging procedure is also presented here. Figure 4-7, demonstrate the SOC estimation by making a comparison between the Simulation results in contrast to the RTDS results, while figure 4-8 illustrate the CC-CV scheme in simulation and compare it to the RTDS results.
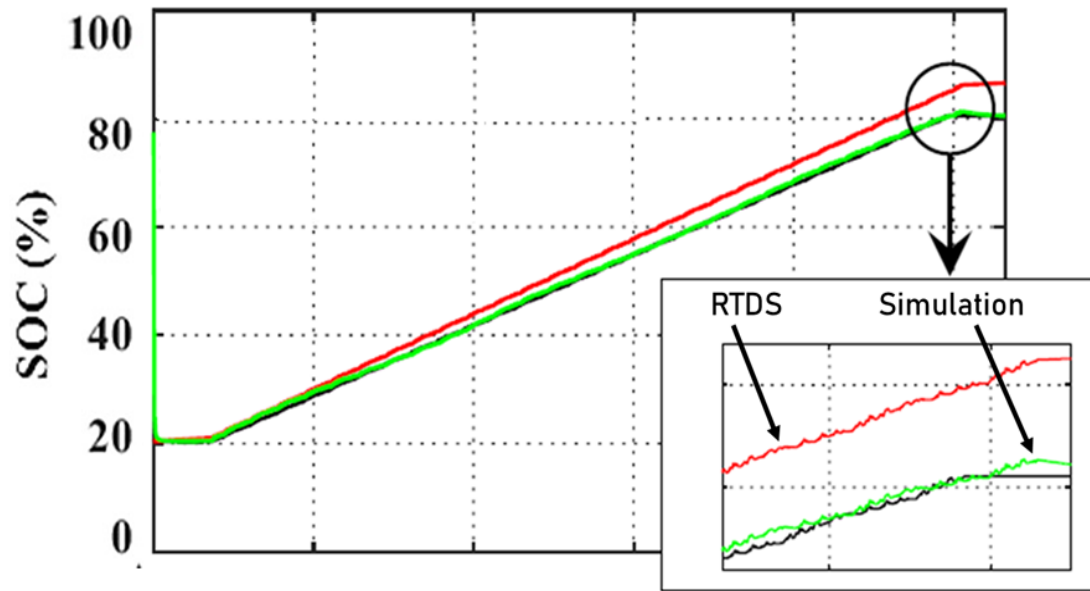
Figure 4-7: SOC Estimation results from the simulation and the RTDS
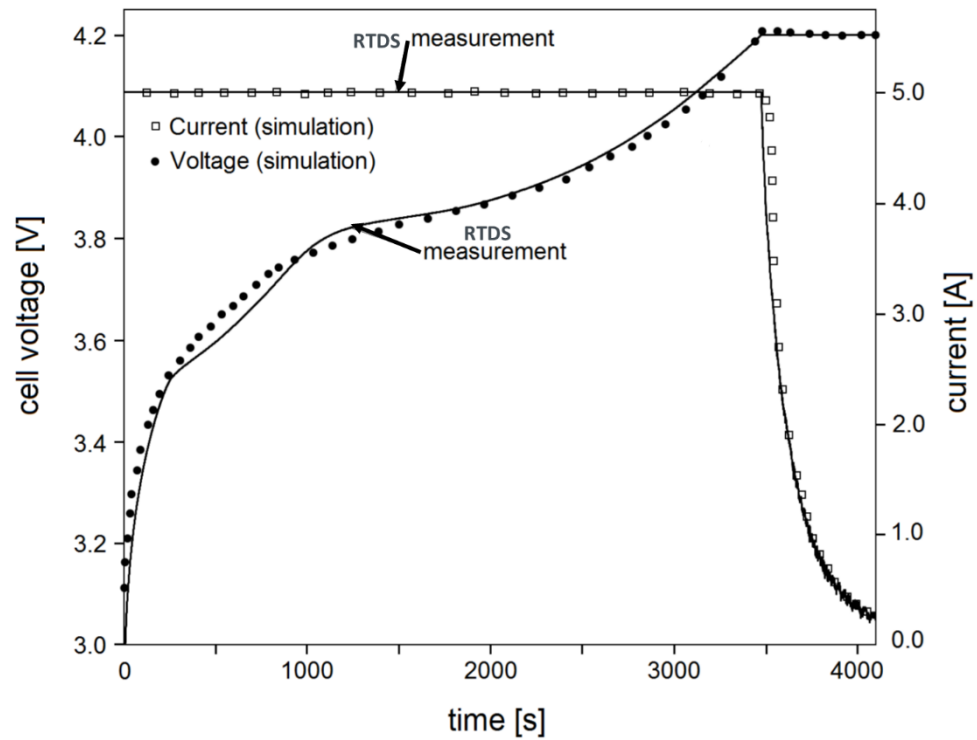

Figure 4-8: Comparison between the Simulation and RTDS results of the CC-CV charging method

In figure 4-7, the system was initiate by a wrong value as before, to study the effectiveness and the quickness in the estimation convergence in the SOC determinations. It evidence that the robustness of the DEKF method had led to fast track and estimating values in both the simulation and RTDS from the beginning within few minutes. It could be noted that, after a reasonable amount of time, and after almost 80% of the SOC, the RTDS values showed a little divergence from the simulation values. This feature may have happened because of the fact that the system has now went from the flat region of charging which from 20-80% to the exponential part from the 80% onwards, and that was predicted, and it was shown clearly in the RTDS results because it's almost as identical as the real life, and it's done in real time, while that incident was not clearly shown in the perfect environment of the simulation. Nevertheless, in general, it could be stated that the proposed model had shown a remarkable outcome in both environment with a maximum mismatch of around 2% in the RTDS results.

Figure 4-8 conclude the desired outcome from this research, which is being able to estimate the value of the SOC in order to use that in the controller to perform the CC-CV charging scheme. The procedure starts by 1C constant current, while the voltage was increasing steadily, then followed by a 4.2 V through the remaining of the charging process, and the overall shape of the curve was like the typical CC-CV curve as mentioned in 2.2.2.

As expected, the RTDS results showed a little mismatch, but in overall it could be neglected since in general the simulation and the RTDS outcomes followed the same pattern throughout the period of the experiment.

CHAPTER 5

CONCLUSION & FUTURE WORK

5.1   Conclusion

This aim of this work was to develop and implement a robust reliable battery management system, that is able to identify the battery parameter, hence calculating its state of charge, which result in optimum control on the charging process.

The proposed model was obtained by combining detailed knowledge of the batteries from all the aspect, starting by the models, and ending by the technique of charging.

Considering one of the most complex and sophisticated battery model, the second order RC secret, lead to produce noteworthy and outstanding results. The model takes into account all the important parameters, which lead to great estimation and outcomes throughout the work.

The introduction of the Double Extended Kalman Filter (DEKF), had enhanced the overall management system throughout its all tasks, whether it's the estimation of the SOC or even in the identification of the battery parameters.

At the end, the CC-CV method was applied using the proposed method with the combination of the selected model, along with the power of the DEKF, which resemble in an acceptable mismatch between the simulation and the RTDS results, and that's demonstrates satisfactory performance by the proposed controllers.

By starting of the validation of the chosen model, throughout the State of Charge (SOC) estimation, and ending with the charging procedure, this work has shown a comprehensive study regarding the enhancing of battery management systems.

5.2   Future Work

Even thought, the proposed method has shown promising results, however, it's worth to mentions that, some aspects that might be considered in future for further study are presented as follows:

- The effect of the temperature in the SOC estimation, was ignored in this work. But it's a rising area of research for the upcoming years. The effect of the temperature could also be implied in the identification of the parameters of the battery, especially if the model become more complex, with addition of more resistors, which will lead to more losses, and the effect of heat could lead to misleading measurements if the used sensors were not sensitive enough.

- In the battery model identification, the capacitors results were always having a little bit percentage of error, more the than the resistor, this could be happened due to the nonlinear nature of the capacitor, or/and the differential equation that would represent the capacitor in the estimation process. And since the supercapacitor are the new era of the storage devices, the upcoming decades will have an enormous research in advancing the nature of the capacitor, and its overall functionality in the power system application.

References

[1]   R. R. Gogula, "A sustainable hybrid/ off grid power generation systems suitable for a remote coastal area in Oman," 2015 IEEE 8th GCC Conference & Exhibition, Muscat, 2015, pp. 1-6.

[2]   M. S. Alam and D. W. Gao, "Modeling and Analysis of a Wind/PV/Fuel Cell Hybrid Power System in HOMER," 2007 2nd IEEE Conference on Industrial Electronics and Applications, Harbin, 2007, pp. 1594-1599.

[3]   A. T. Mohamed, M. A. M. Salim and M. M. Almuhaini, "Reliability assessment and feasibility study for an industrial facility with the integration of hybrid renewable energy system," 2017 International Conference on Communication, Control, Computing and Electronics Engineering (ICCCCEE), Khartoum, 2017, pp. 1-6.

[4]   "Best phone battery life 2018." [Online].

 Available: http://www.expertreviews.co.uk/mobile-phones/1402071/best-phone-battery-life. [Accessed: 20-Mar-2018].

[5]   "Recent Electric Vehicles," in Electric Vehicle Technology Explained, Chichester, UK: John Wiley & Sons, Ltd, 2012, pp. 271–290.

[6]   Y. Wang, Z. Han and J. Shi, "One cell Lithium-ion battery protection IC," 2014 9th IEEE Conference on Industrial Electronics and Applications, Hangzhou, 2014, pp. 1427-1432.

[7]   Z. Ye, X. Wu, Y. Sun and J. Lu, "A Universal Protection Controller for Li-ion Battery Charger," 2010 Asia-Pacific Power and Energy Engineering Conference, Chengdu, 2010, pp. 1-4.

[8]   Z. Rao and S. Wang, "A review of power battery thermal energy management", Renewable and Sustainable Energy Reviews, vol. 15, no. 9, pp. 4554-4571, 2011.

[9]   C. Fleischer, W. Waag, H. Heyn and D. Sauer, "On-line adaptive battery impedance parameter and state estimation considering physical principles in reduced order equivalent circuit battery models", Journal of Power Sources, vol. 260, pp. 276-291, 2014.

[10]   D. V. Cadar, D. M. Petreus, and C. A. Orian, "A method of determining a lithium-ion battery's state of charge," in 2009 15th International Symposium for Design and Technology of Electronics Packages (SIITME), pp. 257–260, 2009.

[11]   R. Hu, "Battery Management System For Electric Vehicle Applications,", M.A.Sc dissertation, Dept. Electrical and Computer Engineering, University of Windsor. 2011.

[12]   H. Chen, T. Cong, W. Yang, C. Tan, Y. Li and Y. Ding, "Progress in electrical energy storage system: A critical review", Progress in Natural Science, vol. 19, no. 3, pp. 291-312, 2009.

[13]   K. Divya and J. Østergaard, "Battery energy storage technology for power systems—An overview", Electric Power Systems Research, vol. 79, no. 4, pp. 511-520, 2009.

[14] X. Luo, J. Wang, M. Dooner and J. Clarke, "Overview of current development in electrical energy storage technologies and the application potential in power system operation", Applied Energy, vol. 137, pp. 511-536, 2015.

[15] A. Satapathy, M. Das, and A. Samanta, "A Comprehensive Study on Battery Management System and Dynamic Analysis of Lithium Polymer Battery," , M.Tech. dissertation, Dept. of Electrical Engineering, National Institute of Technology Rourkela,2016.

[16] L. Lu, X. Han, J. Li, J. Hua, and M. Ouyang, "A review on the key issues for lithium-ion battery management in electric vehicles," J. Power Sources, vol. 226, pp. 272–288, 2013.

[17] "Lithium Battery Failures." [Online]. Available: http://www.mpoweruk.com/lithium_failures.htm. [Accessed: 02-Jan-2017].

[18] L. Maharjan, S. Inoue, H. Akagi and J. Asakura, "State-of-Charge (SOC)-Balancing Control of a Battery Energy Storage System Based on a Cascade PWM Converter," in IEEE Transactions on Power Electronics, vol. 24, no. 6, pp. 1628-1636, June 2009.

[19] J. Lee, O. Nam and B. Cho, "Li-ion battery SOC estimation method based on the reduced order extended Kalman filtering", Journal of Power Sources, vol. 174, no. 1, pp. 9-15, 2007.

[20] T. Hansen and C. J. Wang, "Support vector based battery state of charge estimator," J. Power Sources, vol. 141, no. 2, pp. 351–358, 2005.

[21]   J. Wang, B. Cao, Q. Chen, and F. Wang, "Combined state of charge estimator for electric vehicle battery pack," Control Eng. Pract., vol. 15, no. 12, pp. 1569–1576, 2007.

[22]   C. Zhang, J. Jiang, L. Zhang, S. Liu, L. Wang, and P. C. Loh, "A generalized SOC-OCV model for lithium-ion batteries and the SOC estimation for LNMCO battery," Energies, vol. 9, no. 11, 2016.

[23]   J. H. Aylor, A. Thieme and B. W. Johnso, "A battery state-of-charge indicator for electric wheelchairs," in IEEE Transactions on Industrial Electronics, vol. 39, no. 5, pp. 398-409, Oct. 1992.

[24]   Y. Yang, J. Liu, and C. Tsai, "Improved estimation of residual capacity of batteries for electric vehicles," J. Chinese Inst. Eng., vol. 31, no. 2, pp. 313–322, Mar. 2008.

[25]   V. Pop, H. Bergveld, D. Danilov, and P. Regtien, "Battery management systems: Accurate state-of-charge indication for battery-powered applications", Springer. 2008.

[26]   V. Coroban, I. Boldea and F. Blaabjerg, "A novel on-line state-of-charge estimation algorithm for valve regulated lead-acid batteries used in hybrid electric vehicles," 2007 International Aegean Conference on Electrical Machines and Power Electronics, Bodrum, pp. 39-46, 2007.

[27]   H.J. Bergveld , V. Pop , P.H.L. Notten, "Method of estimating the State-of-Charge and of the use time left of a rechargeable battery, and apparatus for executing such a method", U.S. Patent Application 10/598,038, filed June 26, 2008.

[28]   H. Blanke, O. Bohlen, S. Buller, R. De Doncker, B. Fricke, A. Hammouche, D. Linzen, M. Thele and D. Sauer, "Impedance measurements on lead–acid batteries for state-of-charge, state-of-health and cranking capability prognosis in electric and hybrid electric vehicles", Journal of Power Sources, vol. 144, no. 2, pp. 418-425, 2005.

[29]   S. Rodrigues, N. Munichandraiah and A. Shukla, "A review of state-of-charge indication of batteries by means of a.c. impedance measurements", Journal of Power Sources, vol. 87, no. 1-2, pp. 12-20, 2000.

[30]   J. Xu, C. Mi, B. Cao and J. Cao, "A new method to estimate the state of charge of lithium-ion batteries based on the battery impedance model", Journal of Power Sources, vol. 233, pp. 277-284, 2013.

[31]   W. Waag, S. Käbitz and D. Sauer, "Experimental investigation of the lithium-ion battery impedance characteristic at various conditions and aging states and its influence on the application", Applied Energy, vol. 102, pp. 885-897, 2013.

[32]   S. Nejad, D. T. Gladwin and D. A. Stone, "Sensitivity of lumped parameter battery models to constituent parallel-RC element parameterisation error," IECON 2014 - 40th Annual Conference of the IEEE Industrial Electronics Society, Dallas, TX, 2014, pp. 5660-5665.

[33]   R. Xiong, H. He, F. Sun, X. Liu and Z. Liu, "Model-based state of charge and peak power capability joint estimation of lithium-ion battery in plug-in hybrid electric vehicles", Journal of Power Sources, vol. 229, pp. 159-169, 2013.

[34]   J. Li, J. Klee Barillas, C. Guenther and M. Danzer, "A comparative study of state of charge estimation algorithms for LiFePO4 batteries used in electric vehicles", Journal of Power Sources, vol. 230, pp. 244-250, 2013.

[35]   H. He, R. Xiong and J. Fan, "Evaluation of Lithium-Ion Battery Equivalent Circuit Models for State of Charge Estimation by an Experimental Approach", Energies, vol. 4, no. 4, pp. 582-598, 2011.

[36]   M. Coleman, C. K. Lee, C. Zhu and W. G. Hurley, "State-of-Charge Determination From EMF Voltage Estimation: Using Impedance, Terminal Voltage, and Current for Lead-Acid and Lithium-Ion Batteries," in IEEE Transactions on Industrial Electronics, vol. 54, no. 5, pp. 2550-2557, Oct. 2007.

[37]   F. Baronti, G. Fantechi, L. Fanucci, E. Leonardi, R. Roncella, R. Saletti, S. Saponara, "State-of-charge estimation enhancing of lithium batteries through a temperature-dependent cell model," 2011 International Conference on Applied Electronics, Pilsen, 2011, pp. 1-5.

[38]   F. Auger, M. Hilairet, J. M. Guerrero, E. Monmasson, T. Orlowska-Kowalska and S. Katsura, "Industrial Applications of the Kalman Filter: A Review," in IEEE Transactions on Industrial Electronics, vol. 60, no. 12, pp. 5458-5471, Dec. 2013

[39]   C. R. Gould, C. M. Bingham, D. A. Stone and P. Bentley, "New Battery Model and State-of-Health Determination Through Subspace Parameter Estimation and State-Observer Techniques," in IEEE Transactions on Vehicular Technology, vol. 58, no. 8, pp. 3905-3916, Oct. 2009.

[40] A. El Mejdoubi, A. Oukaour, H. Chaoui, H. Gualous, J. Sabor and Y. Slamani, "State-of-Charge and State-of-Health Lithium-Ion Batteries' Diagnosis According to Surface Temperature Variation," in IEEE Transactions on Industrial Electronics, vol. 63, no. 4, pp. 2391-2402, April 2016.

[41] Z. Chen, Y. Fu and C. C. Mi, "State of Charge Estimation of Lithium-Ion Batteries in Electric Drive Vehicles Using Extended Kalman Filtering," in IEEE Transactions on Vehicular Technology, vol. 62, no. 3, pp. 1020-1030, March 2013.

[42] R. Xiong, F. Sun, Z. Chen and H. He, "A data-driven multi-scale extended Kalman filtering based parameter and state estimation approach of lithium-ion olymer battery in electric vehicles", Applied Energy, vol. 113, pp. 463-476, 2014.

[43] C. Hu, B. Youn and J. Chung, "A multiscale framework with extended Kalman filter for lithium-ion battery SOC and capacity estimation", Applied Energy, vol. 92, pp. 694-704, 2012.

[44] X. Hu, S. Li, H. Peng and F. Sun, "Robustness analysis of State-of-Charge estimation methods for two types of Li-ion batteries", Journal of Power Sources, vol. 217, pp. 209-219, 2012.

[45] J. Kim and B. H. Cho, "State-of-Charge Estimation and State-of-Health Prediction of a Li-Ion Degraded Battery Based on an EKF Combined with a Per-Unit System," in IEEE Transactions on Vehicular Technology, vol. 60, no. 9, pp. 4249-4260, Nov. 2011.

[46]   J. Kim, S. Lee and B. H. Cho, "Complementary Cooperation Algorithm Based on DEKF Combined With Pattern Recognition for SOC/Capacity Estimation and SOH Prediction," in IEEE Transactions on Power Electronics, vol. 27, no. 1, pp. 436-451, Jan. 2012.

[47]   S. Yuan, H. Wu and C. Yin, "State of Charge Estimation Using the Extended Kalman Filter for Battery Management Systems Based on the ARX Battery Model", Vol. 6, No. 1, pp. 444-470, 2016.

[48]   B. S. Bhangu, P. Bentley, D. A. Stone and C. M. Bingham, "Observer techniques for estimating the state-of-charge and state-of-health of VRLABs for hybrid electric vehicles," 2005 IEEE Vehicle Power and Propulsion Conference, Chicago, IL, 2005.

[49]   Z. He, M. Gao, C. Wang, L. Wang and Y. Liu, "Adaptive State of Charge Estimation for Li-Ion Batteries Based on an Unscented Kalman Filter with an Enhanced Battery Model", Vol.6, No.8, pp 4134-4151, 2013.

[50]   H. Aung, K. Soon Low and S. Ting Goh, "State-of-Charge Estimation of Lithium-Ion Battery Using Square Root Spherical Unscented Kalman Filter (Sqrt-UKFST) in Nanosatellite," in IEEE Transactions on Power Electronics, vol. 30, no. 9, pp. 4774-4783, Sept. 2015.

[51]   G. Plett, "Sigma-point Kalman filtering for battery management systems of LiPB-based HEV battery packs", Journal of Power Sources, vol. 161, no. 2, pp. 1369-1384, 2006.

[52]   J. Meng, G. Luo and F. Gao, "Lithium Polymer Battery State-of-Charge Estimation Based on Adaptive Unscented Kalman Filter and Support Vector Machine," in IEEE Transactions on Power Electronics, vol. 31, no. 3, pp. 2226-2238, March 2016.

[53]   A. Zenati, P. Desprez and H. Razik, "Estimation of the SOC and the SOH of li-ion batteries, by combining impedance measurements with the fuzzy logic inference," IECON 2010 - 36th Annual Conference on IEEE Industrial Electronics Society, Glendale, AZ, pp. 1773-1778, 2010.

[54]   C. Hametner and S. Jakubek, "State of charge estimation for Lithium Ion cells: Design of experiments, nonlinear identification and fuzzy observer design", Journal of Power Sources, vol. 238, pp. 413-421, 2013.

[55]   W. Chang, "Estimation of the state of charge for a LFP battery using a hybrid method that combines a RBF neural network, an OLS algorithm and AGA", International Journal of Electrical Power & Energy Systems, vol. 53, pp. 603-611, 2013.

[56]   X. Chen, W. Shen, M. Dai, Z. Cao, J. Jin and A. Kapoor, "Robust Adaptive Sliding-Mode Observer Using RBF Neural Network for Lithium-Ion Battery State of Charge Estimation in Electric Vehicles," in IEEE Transactions on Vehicular Technology, vol. 65, no. 4, pp. 1936-1947, April 2016.

[57]   A. Jossen, "Fundamentals of battery dynamics", Journal of Power Sources, vol. 154, no. 2, pp. 530-538, 2006.

[58] J. Remmlinger, M. Buchholz, T. Soczka-Guth and K. Dietmayer, "On-board state-of-health monitoring of lithium-ion batteries using linear parameter-varying models", Journal of Power Sources, vol. 239, pp. 689-695, 2013.

[59] Z. He, Y. Liu, M. Gao and Caisheng Wang, "A joint model and SOC estimation method for lithium battery based on the sigma point KF," 2012 IEEE Transportation Electrification Conference and Expo (ITEC), Dearborn, MI, pp. 1-5, 2012.

[60] P. Gregory,"Dual and joint EKF for simultaneous SOC and SOH estimation." In Proceedings of the 21st Electric Vehicle Symposium (EVS21), Monaco, pp. 1-12. 2005.

[61] G. Plett, "Recursive approximate weighted total least squares estimation of battery cell total capacity", Journal of Power Sources, vol. 196, no. 4, pp. 2319-2331, 2011.

[62] X. Hu, F. Sun, Y. Zou and H. Peng, "Online estimation of an electric vehicle Lithium-Ion battery using recursive least squares with forgetting," Proceedings of the 2011 American Control Conference, San Francisco, CA, pp. 935-940, 2011.

[63] H. He, X. Zhang, R. Xiong, Y. Xu and H. Guo, "Online model-based estimation of state-of-charge and open-circuit voltage of lithium-ion batteries in electric vehicles", Energy, vol. 39, no. 1, pp. 310-318, 2012.

[64] T. Kim and W. Qiao, "A Hybrid Battery Model Capable of Capturing Dynamic Circuit Characteristics and Nonlinear Capacity Effects," in IEEE Transactions on Energy Conversion, vol. 26, no. 4, pp. 1172-1180, Dec. 2011.

[65] E. Krüger, Q. T. Tran and K. Mamadou, "Normalized least mean squares observer for battery parameter estimation," 2015 IEEE Eindhoven PowerTech, Eindhoven, pp. 1-6, 2015.

[66] Li Xue, Jiang Jiuchun, Zhang Caiping, Zhang Weige and Sun Bingxiang, "Effects analysis of model parameters uncertainties on battery SOC estimation using H-infinity observer," 2014 IEEE 23rd International Symposium on Industrial Electronics (ISIE), Istanbul, pp. 1647-1653, 2014.

[67] I. Kim, "The novel state of charge estimation method for lithium battery using sliding mode observer", Journal of Power Sources, vol. 163, no. 1, pp. 584-590, 2006.

[68] P. Kumar and P. Bauer, "Parameter extraction of battery models using multiobjective optimization genetic algorithms," Proceedings of 14th International Power Electronics and Motion Control Conference EPE-PEMC, Ohrid, pp. 106-110, 2010.

[69] X. Hu, S. Li and H. Peng, "A comparative study of equivalent circuit models for Li-ion batteries", Journal of Power Sources, vol. 198, pp. 359-367, 2012.

[70] H. Shareef, M. M. Islam, and A. Mohamed, "A review of the stage-of-the-art charging technologies, placement methodologies, and impacts of electric vehicles," Renew. Sustain. Energy Rev., vol. 64, pp. 403–420, 2016.

[71] J. Y. Yong, V. K. Ramachandaramurthy, K. M. Tan, and N. Mithulananthan, "A review on the state-of-the-art technologies of electric vehicle, its impacts and prospects," Renewable. Sustainable Energy., vol. 49, pp. 365–385, 2015.

[72] C. H. Dharmakeerthi, N. Mithulananthan and T. K. Saha, "Modeling and planning of EV fast charging station in power grid," 2012 IEEE Power and Energy Society General Meeting, San Diego, CA, pp. 1-8, 2012

[73] Chih-Chiang Hua and Meng-Yu Lin, "A study of charging control of lead-acid battery for electric vehicles," ISIE'2000. Proceedings of the 2000 IEEE International Symposium on Industrial Electronics (Cat. No.00TH8543), Cholula, Puebla, Mexico, pp. 135-140 vol.1, 2000.

[74] "Battery Chargers and Charging Methods." [Online]. Available: http://www.mpoweruk.com/chargers.htm#pulse. [Accessed: 13-Nov-2016].

[75] S. Li, C. Zhang, and S. Xie, "Research on fast charge method for lead-acid electric vehicle batteries," 2009 Int. Work. Intell. Syst. Appl. ISA 2009, pp. 1–5, 2009.

[76] N., Tho, and Linda Bushnell. "Advanced Battery Charging Techniques: Pulse-Charging in Large-Scale Applications-Design of Divide and Conquer Technique for High-Capacity Batteries." Technical Report (2003).

[77] L. Chen, "Design of Duty-Varied Voltage Pulse Charger for Improving Li-Ion Battery-Charging Response," in IEEE Transactions on Industrial Electronics, vol. 56, no. 2, pp. 480-487, Feb. 2009.

[78] Y. S. Chu, R. Y. Chen, T. J. Liang, S. K. Changchien and J. F. Chen, "Positive/negative pulse battery charger with energy feedback and power factor correction," Twentieth Annual IEEE Applied Power Electronics Conference and Exposition,. APEC 2005., Austin, TX, Vol. 2, pp. 986-990, 2005.

[79] S. Falahati, S. A. Taher, and M. Shahidehpour, "A new smart charging method for EVs for frequency control of smart grid," Int. J. Electronics. Power Energy Syst., vol. 83, pp. 458–469, 2016.

[80] S. Malkhandi, "Fuzzy logic-based learning system and estimation of state-of-charge of lead-acid battery", Engineering Applications of Artificial Intelligence, vol. 19, no. 5, pp. 479-485, 2006.

[81] S. A. Taher, M. Hajiakbari Fini, and S. Falahati Aliabadi, "Fractional order PID controller design for LFC in electric power systems using imperialist competitive algorithm," Ain Shams Eng. J., vol. 5, no. 1, pp. 121–135, 2014.

[82] I. G. Damousis, A. G. Bakirtzis and P. S. Dokopoulos, "A solution to the unit-commitment problem using integer-coded genetic algorithm," in IEEE Transactions on Power Systems, vol. 19, no. 2, pp. 1165-1172, May 2004.

[83] B. Yagcitekin and M. Uzunoglu, "A double-layer smart charging strategy of electric vehicles taking routing and charge scheduling into account," Appl. Energy, vol. 167, pp. 407–419, 2016.

[84] A. S. Masoum, S. Deilami, P. S. Moses, M. A. S. Masoum, and A. Abu-Siada, "Smart load management of plug-in electric vehicles in distribution and residential networks with charging stations for peak shaving and loss minimisation considering voltage regulation," IET Gener. Transm. Distrib., vol. 5, no. 8, p. 877, 2011.

[85] A. D. Hilshey, P. Rezaei, P. D. H. Hines and J. Frolik, "Electric vehicle charging: Transformer impacts and smart, decentralized solutions," 2012 IEEE Power and Energy Society General Meeting, San Diego, CA, pp. 1-8, 2012.

[86] M. A. S. Masoum, P. S. Moses, and S. Hajforoosh, "Distribution transformer stress in smart grid with coordinated charging of plug-in electric vehicles," 2012 IEEE PES Innovation. Smart Grid Technol. ISGT 2012, pp. 1–8, 2012.

[87] G. Razeghi, L. Zhang, T. Brown, and S. Samuelsen, "Impacts of plug-in hybrid electric vehicles on a residential transformer using stochastic and empirical analysis," J. Power Sources, vol. 252, pp. 277–285, 2014.

[88] E. Ramos Muñoz, G. Razeghi, L. Zhang, and F. Jabbari, "Electric vehicle charging algorithms for coordination of the grid and distribution transformer levels," Energy, vol. 113, pp. 930–942, 2016.

Vitae

Name   :   Abdelhamed Tarig Abdelhamed Mohamed

Nationality   :   Sudanese

Date of Birth   :   3/25/1992

Email   :   a.hameedtarig@gmail.com

Address   : Khartoum, Sudan, postal code: 11112

Academic Background   : **M.Sc. (Electrical Engineering), May 2018**

                                        King Fahd University of Petroleum and Minerals

                                        Dhahran, Saudi Arabia

                                        B.Sc. (Electrical Engineering), October 2014

                                        University of Khartoum, Sudan, 2014

                                        Khartoum, Sudan

Publications   : "Reliability Assessment and Feasibility Study for an Industrial Facility with the Integration of Hybrid Renewable Energy System", Abdelhamed T. Mohamed, Mohammed Al-Hassan M. Salim, Mohammad M. Almuhaini, International Conference on Communication, Control, Computing and Electronics Engineering (ICCCCEE), Khartoum, Sudan, 2017.

"Characterization and Implementation of Battery Management System", Abdelhamed T. Mohamed and Mohammad A. Abido, Journal paper, to be submitted.

"Electrical Characterization and Financial Viability of a Diesel -PV-Wind Hybrid Power System with the Addition of Storage Devices for a Remote Area", Abdelhamed T. Mohamed and Ahmed Mohamed, Smart Cities Symposium, Manama, Bahrain, 2018.